Cedar Lake, Wisconsin - Limnological response to alum treatment: 2021 interim report

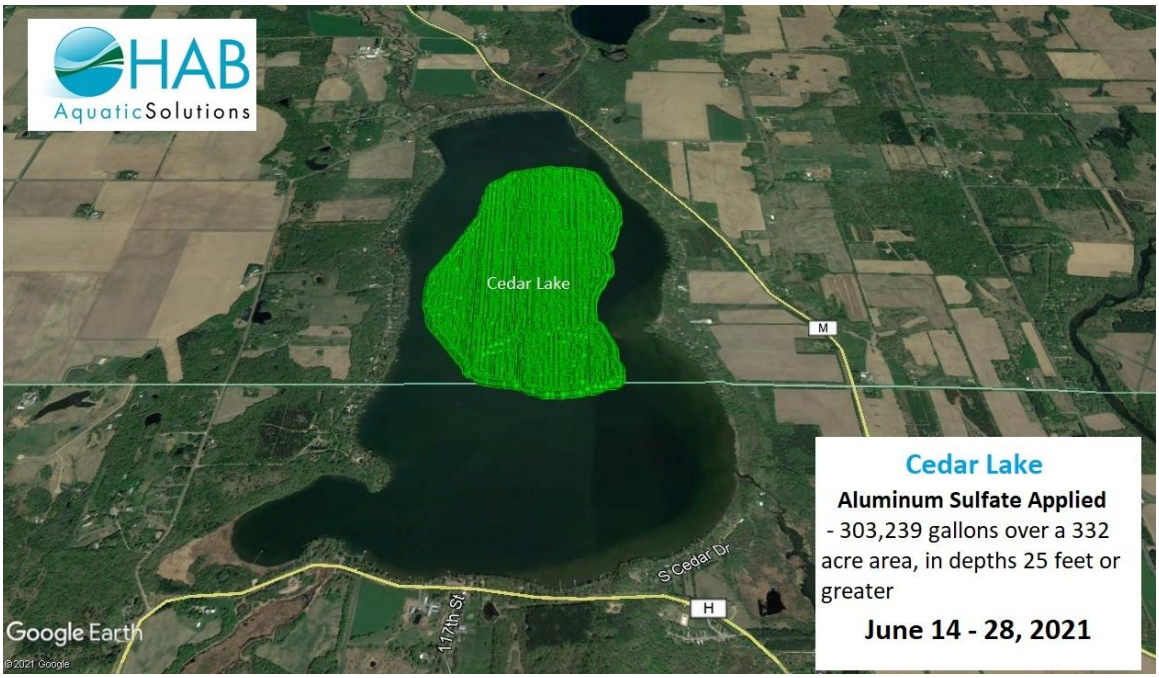

Aerial map of alum application to Cedar Lake in 2021. Credits: HAB Aquatic Solutions, St. Paul, MN

31 January 2022

University of Wisconsin – Stout
Sustainability Sciences Institute - Center for Limnological Research and Rehabilitation
Department of Biology
123E Jarvis Hall
Menomonie, Wisconsin 54751
715-338-4395
jamesw@uwstout.edu

Harmony Environmental
516 Keller Ave S
Amery, Wisconsin 54001
715-268-9992
harmonyenv@amerytel.net

Executive Summary

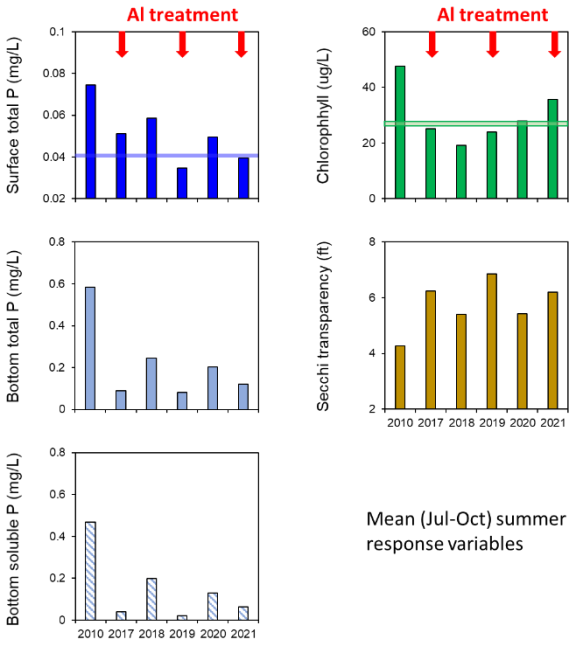

A comparison of mean summer (July-early October) summer concentrations of surface and bottom total phosphorus (P) and soluble reactive P (SRP), chlorophyll and Secchi transparency during a pretreatment year (2010) and the post-treatment years 2017-21.

- In 2021, an unusually early spring and ice out coincided with early stratification and the development of bottom anoxia in May coupled with modest internal P loading from sediment before the June alum treatment. Mixing in early June was followed by the development of a metalimnetic algal bloom and subsurface (4-5 m) chlorophyll concentration maximum in late June-early July that was dominated by the cyanobacteria *Aphanizomenon flos-aquae* and *Woronichinia naegeliana*. Additional mixing of modest internal P loading during the onset of Fall overturn in August coincided with the development of an algal bloom dominated by the same *W. naegeliana* cyanobacteria and chlorophyll peaks in excess of 60 µg/L in early September.
- The alum application in 2021 occurred between 14 and 28 June. An ~ 50 g/m^2 Al dose was applied to sediments within the > 25-ft depth contour to suppress internal P loading from these anoxic sediments.
- Mean summer (JUL-early OCT) bottom total P and SRP concentrations declined overall in 2021 in conjunction with the alum treatment, representing a 79% and 87% reduction, respectively, compared to 2010. Mean summer surface total P also declined in 2021, relative to 2020 and 2010, to 0.040 mg/L. Unfortunately, mean chlorophyll was much higher at 36 µg/L in 2021 compared to the mean 29 µg/L in 2020, but still 25% lower than the pretreatment average. Finally, mean Secchi transparency was relatively deep in 2021 at 6.2 ft. These patterns reflected the outcome of mixing and transfer of modest bottom P concentrations to the surface and algal uptake after early stratification and bottom anoxia in May 2021, and after the mixing period and onset of Fall turnover in August 2021.

- After 2 partial alum treatments to the sediment contained within the 20-ft to 25-ft depth contour and 3 alum applications to sediments contained with the > 25-ft depth contour, laboratory-derived anaerobic diffusive P flux has improved by 44% to 96% in 2021 versus 2017 (i.e., immediately before the first Al application). Diffusive P flux loading reduction since 2017 is a mean 79% for sediments within the > 25-ft depth contour and 59% for sediments within the 20-ft to 25-ft depth contour.

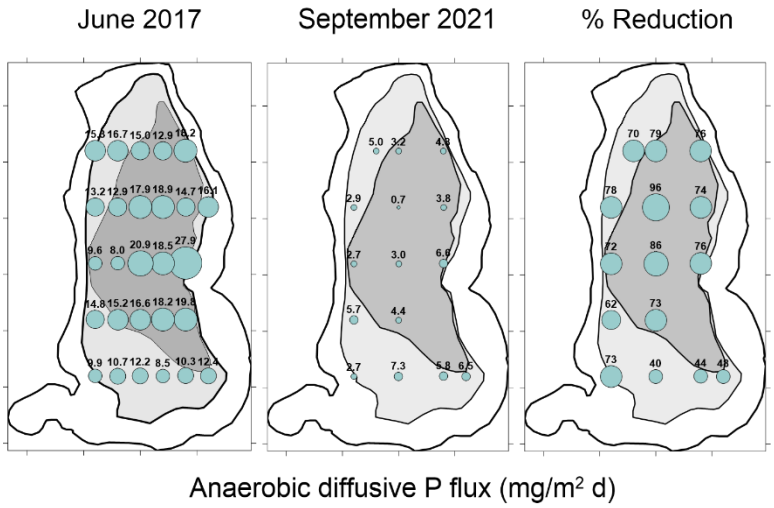

Spatial variations in laboratory-derived anaerobic diffusive phosphorus flux from sediment immediately before (2017) and after alum applications to Cedar Lake. The light gray area was treated with 20 g Al/m^2 in 2017 and 2019. The dark gray area was treated with ~26-28 g Al/m^2 in 2017 and 2019 and 50 g Al/m^2 in 2021.

- Total aluminum concentrations have increased in sediments located at depths > 25 ft as a result of the 2021 alum application. Estimation of area-based Al concentration was difficult to evaluate from 10-cm surface sediment core sections because the Al floc layer is situated on top and does not represent the entire 10-cm section. Native (i.e., natural aluminum in the sediment before the alum treatments) sediment Al concentration must be factored out so additional vertical profiles will need to be collected at a subset of stations in June 2022 to more accurately quantify the area-based Al concentration.
- The 4th alum application can be scheduled for as early as 2023. However, Al dosage and treatment areas for this application need to be assessed based on findings from the monitoring study to be conducted in 2022. Do we continue to treat only the sediment contained within the > 25-ft depth contour with the higher Al dose, or go back to the original treatment scenario where sediments within the 20-ft to 25-ft depth contour are treated with a 20 g/m2 dose while sediments within the > 25-ft depth contour are treated with a 26 g/m2 dose? Changes in anaerobic diffusive P flux and Al binding of P in the sediment as well as limnological response such as bottom P, surface P, and chlorophyll concentration patterns in 2022 will be critical considerations in the alum dose and

application decision-making process for 2023.

Objectives

Multiple Al applications over a period of 10-12 years are planned for Cedar Lake in order to control internal phosphorus loading. It is critical to conduct post-treatment monitoring of water and sediment chemistry to document the trajectory of water quality improvement during rehabilitation to make informed decisions regarding adjusting management to meet future water quality goals. Post-treatment monitoring included field and laboratory research to document changes in 1) hydrology and watershed phosphorus (P) loading, 2) the P budget and lake water quality, 3) binding of sediment mobile P fractions that have contributed to internal P loading by alum, and 4) rates of diffusive P flux from the sediment under anaerobic conditions. Overall, lake water quality is predicted to respond to watershed and internal P loading reduction with lower surface concentrations of total P and chlorophyll concentrations throughout the summer, lower bloom frequency of nuisance chlorophyll levels, and higher water transparency. Multiple Al applications between 2017 and 2029 should result in the binding of iron-bound P and substantial reduction in diffusive P flux from sediments under anaerobic conditions (i.e., internal P loading).

The first alum application occurred in late June 2017. The Al concentration was 20 g/m^2 for sediment located within the 20-25 ft depth contour and 26 g/m^2 for sediment located at depths > 25 ft. The second alum application occurred during 11-22 June 2019 and Al concentrations ranged between 22 g/m^2 within the 20-25 ft depth contour and ~ 28 g/m^2 for depths > 25 ft. This combined Al application of 42 g/m^2 and 54 g/m^2 to the two depth zones ideally represented ~ 42% of the target Al doses of 100 g/m^2 and 130 g/m^2. However, sediment monitoring suggested the Al floc had spread and become diluted particularly at depths > 25 ft, resulting in lower measured Al concentrations than predicted. Lower Al recovery might be attributed to Al floc movement or redistribution and spread during and after application by wind activity and water currents. Al floc movement during settling is not uncommon and has been reported to occur in other alum treatments (Egemose et al. 2009, 2013; Huser 2017; James and Bischoff 2020). As an adaptive management decision, the third alum treatment in June 2021 was applied to sediments located at depths > 25 ft only to increase the overall Al concentration and thickness of the Al floc in this deeper area of the lake. Since this area is smaller than the earlier combined application

area encompassing depths > 20 ft (332 ac), the Al dosage was increased to ~ 50 g/m^2 within the > 25-ft zone without increasing overall costs.

The objectives of this interim report were to describe the 2021 limnological and sediment variable response to these alum treatments in Cedar Lake. Limnological monitoring is being used in conjunction with an adaptive management approach to gauge lake response and the need, if any, to adjust Al dose or application strategy.

Methods

Alum application in 2021

Alum (aluminum sulfate) was applied to Cedar Lake by HAB Aquatic Solutions (St. Paul, MN) between 14 and 28 June 2021. The Al dosage was 50 g/m^2 (913 gal/ac) to depths > the 25-ft contour (see cover photo).

Watershed loading and lake monitoring

A gauging station was established on Horse Creek above Cedar Lake at 10th Ave for concentration, loading, and flow determination between May and October 2021 (Fig. 1). Unfortunately, the flow velocity equipment was vandalized and destroyed in late July 2021. Grab samples were collected biweekly at the 10th Ave gauging station for chemical analysis. Additional samples were collected biweekly at a Horse Creek station on County Y, located below Horse Lake. Water samples were analyzed for total suspended solids (TSS), total volatile solids (VSS), total P, and soluble reactive P (SRP) using standard methods (APHA 2011). Summer tributary P loading was calculated using the computer program FLUX.

The deep basin water quality station WQ 2 was sampled biweekly between May and October 2021 (Fig. 1). An integrated sample over the upper 2-m was collected for analysis of total P, SRP, and chlorophyll a. An additional discrete sample was collected within 0.5 m of the

sediment surface for analysis of total and SRP. Secchi transparency and in situ measurements (temperature, dissolved oxygen, pH, and conductivity) were collected on each date using a YSI 6600 sonde (Yellow Springs Instruments) that was calibrated against dissolved oxygen Winkler titrations (APHA 2011) and known buffer solutions.

Sediment chemistry

Sediment characteristics. A sediment core was collected in September 2021 at WQ 2 (Fig. 1) for determination of vertical profiles of various sediment characteristics and phosphorus fractions (see Analytical methods below). The sediment core was sectioned at 1-cm intervals between 0 and 10 cm and at 2-cm intervals below the 10-cm depth for determination of moisture content, wet and dry bulk density, loss-on-ignition organic matter, loosely-bound P, iron-bound P, labile organic P, aluminum-bound P, and total aluminum. Additional cores were collected 15 stations located along a grid that was established in 2012 (Fig. 1). An upper 10 cm slice was sectioned for the variables listed above. The 8 stations located at depths > 25 ft and 7 stations l established between the 20 ft and 25 ft depth contours were used to evaluate the two alum treatment zones (reported in James 2014).

Laboratory-derived diffusive phosphorus flux from sediments under anaerobic conditions. Anaerobic diffusive P fluxes were measured from intact sediment cores collected at stations shown in Figure 1 in September. Three sediment cores were collected at WQ 2 and one sediment core was collected at each spatial station to monitor alum treatment effectiveness after 2021 alum application. The sediment incubation systems were placed in a darkened environmental chamber and incubated at 20 C for up to 5 days. The incubation temperature was set to a standard temperature for all stations for comparative purposes. The oxidation-reduction environment in each system was controlled by gently bubbling nitrogen through an air stone placed just above the sediment surface to maintain anaerobic conditions.

Water samples for SRP were collected from the center of each system using an acid-washed syringe and filtered through a 0.45 µm membrane syringe filter (Nalge). The water volume removed from each system during sampling was replaced by addition of filtered lake water

preadjusted to the proper oxidation-reduction condition. These volumes were accurately measured for determination of dilution effects. Rates of P release from the sediment (mg/m^2 d) were calculated as the linear change in mass in the overlying water divided by time (days) and the area (m^2) of the incubation core liner. Regression analysis was used to estimate rates over the linear portion of the data.

Analytical methods. A known volume of sediment was dried at 105 ^oC for determination of moisture content, wet and dry bulk density, and burned at 550 ^oC for determination of loss-on-ignition organic matter content (Avnimelech et al. 2001, Håkanson and Jansson 2002). Phosphorus fractionation was conducted according to Hieltjes and Lijklema (1980), Psenner and Puckso (1988), and Nürnberg (1988) for the determination of ammonium-chloride-extractable P (loosely-bound P), bicarbonate-dithionite-extractable P (i.e., iron-bound P), and sodium hydroxide-extractable P (i.e., aluminum-bound P).

The loosely-bound and iron-bound P fractions are readily mobilized at the sediment-water interface as a result of anaerobic conditions that lead to desorption of P from sediment and diffusion into the overlying water column (Mortimer 1971, Boström et al. 1982, Boström 1984, Nürnberg 1988). The sum of the loosely-bound and iron-bound P fraction represents redox-sensitive P (i.e., the P fraction that is active in P release under anaerobic and reducing conditions) and will be referred to as ***redox-P***. Aluminum-bound P reflects P bound to the Al floc after aluminum sulfate application and its chemical transformation to aluminum hydroxide ($Al(OH)_3$).

Summary of Results

Hydrology and phosphorus loading

On an annual basis, precipitation in 2021 was below the~ 33-inch average since 1980 at ~26 inches (Fig. 2). Monthly precipitation was well below the long-term average in June and September 2021 and near the average in July and August (Fig. 3). Horse Creek at 10th Ave summer flow exhibited peaks in May in conjunction with storms with precipitation that ranged

between 0.5 and 1 inch (Fig. 4). Flows subsided during the period of lower precipitation in June. Horse Creek at 10th Ave mean summer (May-October) daily flow was lower relative to most other years at 0.49 m^3/s in 2021 (Fig. 5).

Total P concentrations in Horse Creek at 10th Ave exhibited a ~ 0.10 mg/L peak in late May in conjunction with storm-related flows (Fig. 6). Concentrations declined to ~ 0.04 mg/L during the lower flow period of June, then increased during storm-generated inflows in mid-August. Soluble reactive P concentrations ranged between 0.01 mg/L and 0.03 mg/L. TSS and VSS concentrations were highest in late May at ~42 mg/L and 23 mg/L, respectively, and declined to nominal levels between June and October.

Suspended sediment and P concentrations exhibited a different seasonal pattern in Horse Creek at County Y, located below Horse Lake (Fig. 6). TSS, VSS, and total P exhibited modest concentration peaks in late May to early June compared to the greater concentration increases observed at 10th Ave. In particular, total P concentration peaks were lower at ~ 0.045 mg/L to 0.07 mg/L during this period compared to concentration ranged observed at 10th Ave. In contrast to seasonal patterns observed at 10th Ave, TSS, VSS, and total P concentrations increased to maxima between July and early October at County Y. These summer concentration increases might reflect periods of sediment resuspension during periods of high wind and wave activity in shallow Horse Lake with discharge to Horse Creek. Additionally, SRP concentrations were very low to undetectable at County Y versus 10th Ave. Summer variable concentration differences between the two stations suggested, 1) TSS-VSS concentration peaks at 10th Ave in May probably originated from watershed sources located between Horse Lake and Cedar Lake and this load likely entered Cedar Lake, 2) high TSS-VSS and total P concentrations originating from Horse Lake after July probably settled in the Horse Creek floodplain upstream of Cedar Lake (i.e., County Y TSS-VSS and total P >> 10th Ave TSS-VSS and total P), and 3) SRP loads probably originated downstream of Horse Lake during the summer (i.e., County Y SRP << 10th Ave SRP). Similar upstream-downstream patterns were observed during the 2009-2011 monitoring period (James 2014).

Concentration-flow relationships in 2021 were generally like those observed historically (Fig. 7). Flow-averaged summer (May through July only) total P and SRP in 2021 were 0.082 mg/L and 0.021 mg/L (Table 1). The flow-averaged SRP concentration accounted for ~ 26% of the total P in 2021. Unfortunately, flow information past July was missing as a result of vandalism of the flow logger. Estimation of daily load was, therefore, confined to the period May through July 2021 only.

Table 1. Mean summer (May-October) constituent concentrations and loading for the Horse Creek inflow station at 10th Ave.

Year	Variable	TSS	Total P	SRP
2010	Concentration (mg/L)		0.089	0.031
	Load (kg/d)		4.18	1.42
2017	Concentration (mg/L)	15.2	0.084	0.034
	Load (kg/d)	767.8	4.26	1.71
2018	Concentration (mg/L)	16.5	0.100	0.039
	Load (kg/d)	549	3.36	1.28
2019	Concentration (mg/L)	10.6	0.083	0.035
	Load (kg/d)	524	4.07	1.72
2020	Concentration (mg/L)		0.083	0.033
	Load (kg/d)		6.14	2.35
2021	Concentration (mg/L)[1]	22.1	0.082	0.021
	Load (kg/d)[2]	945	3.49	0.88
			Flow logger vandalized	

[1]Represents a flow-weighted mean between APR-JUL only

[2]Represents an estimated daily load between APR-JUL only

Lake limnological response

An early spring and ice out conditions in 2021 resulted in the development of weak stratification in May (Fig. 8). The bottom waters rapidly became anoxic during this temporary stratification period, resulting in the potential for diffusive P flux from sediment under anaerobic conditions before the mid-June alum treatment. The lake mixed in mid-June, then bottom anoxia redeveloped between early July and the end of August in conjunction with summer stratified conditions. Epilimnetic expansion and thermocline erosion in August resulted in vertical water exchanges and eventually complete water column reoxygenation in September.

Bottom total P and SRP concentrations increased slightly after the establishment of hypolimnetic anoxia in May through mid-June (Fig. 9 and 10, also see Appendix I). For instance, bottom total P increased from 0.048 mg/L in early May to a peak concentration of 0.064 mg/L in mid-June. Bottom SRP increased to 0.036 mg/L in conjunction with bottom anoxia in May. This bottom soluble P pulse developed before the alum treatment and was, thus, potentially available for cyanobacteria uptake. Remarkably, both bottom total P and SRP concentrations increased steadily between early July and mid-August, suggesting the occurrence of some diffusive P flux

after the alum treatment. Concentration maxima were modest at 0.223 mg/L total P and 0.156 mg/L SRP, compared to bottom concentration peaks observed in 2010. Nevertheless, this bottom SRP was potentially available for cyanobacteria uptake when entrained into the surface waters during mixing in August. As discussed below, mixing of this hypolimnetic P into the surface waters during epilimnetic expansion and fall turnover coincided with the development of an algal bloom that exceeded 60 µg/L chlorophyll, suggesting uptake of this P for growth (see Fig. 10 and 12).

Surface total P concentrations declined during and shortly after the alum treatment but then increased linearly between July and mid-September to a peak of 0.074 mg/L. This surface total P peak coincided with peak chlorophyll concentrations, reflecting incorporation of P derived from the hypolimnion into algal biomass (Fig. 12).

A metalimnetic chlorophyl peak exceeding 35 µg/L developed in late June-early July shortly after the alum treatment (Fig. 10 and Appendix I). Mixing of the modest internal P load into the surface waters in June (Fig. 8) and uptake by cyanobacteria for later growth was a plausible explanation for this subsurface peak. The algal assemblage of this metalimnetic peak was dominated by the cyanobacterial species *Aphanizomenon flos-aqua*e and *Woronichinia naegeliana* (Fig. 12). High water clarity and deep light penetration during this period played a role in the positioning of these species since they can adapt to and often prefer lower radiation levels for optimal photosynthesis and growth. They were also positioned immediately above modest hypolimnetic soluble P concentrations and thus had potential access to nutrients for uptake and growth.

Although the algal assemblage was diverse during peak surface biomass in August, the dominant cyanobacterial species was again *W. naegeliana* (Fig. 12 and 13). The August bloom developed shortly after mixing and vertical transport to the surface of modest internal P loads that had accumulated in the hypolimnion between July and early August (Fig. 9 and 10 and Appendix I). Overall, these seasonal patterns suggested that *W. naegeliana* populations took advantage of the May internal P loading period and positioned in the metalimnion in late June-early July where photosynthetically active radiation was optimal and modest hypolimnetic soluble P

concentrations were potentially accessible for uptake. This population (and other species) were mixed into the surface waters in early August with concomitant available SRP from the bottom waters. Uptake of this internal P load was accompanied by a bloom with uniform chlorophyll concentration exceeding 60 µg/L throughout the water column that extended into September (Fig. 10 and Appendix I).

Secchi transparency was very high during the period of relatively low chlorophyll concentrations in May through mid-July then declined steadily to ~ 1 m in association with the chlorophyll peak in mid-August through October (Fig. 14). Secchi transparency exhibited a significant inverse pattern to that of chlorophyll, indicating that light extinction was due to algae versus inorganic turbidity (Fig. 15).

A comparison of mean summer (July-early October) limnological response variables before alum treatment (i.e., 2010) versus 2021 is shown in Figure 16 and Table 2. Mean bottom total P and SRP concentrations declined overall in 2021 in conjunction with the alum treatment (Fig. 16), representing a 79% and 87% reduction, respectively, compared to 2010 (Table 2). Mean summer surface total P also declined in 2021, relative to 2020 and 2010, to 0.040 mg/L (Table 2). Unfortunately, mean chlorophyll was much higher at 36 µg/L in 2021 compared to the mean 29 µg/L in 2020, but still 25% lower than the pretreatment average. Finally, mean Secchi transparency was relatively deep in 2021 at 6.2 ft (Fig. 16 and Table 2). These patterns reflected the outcome of mixing and transfer of modest bottom P concentrations to the surface and algal uptake after early stratification and bottom anoxia in May 2021, and after the mixing period and onset of Fall turnover in August 2021.

Table 2. Summary of changes in lake water quality and sediment variables after the initial alum treatment in June 2017. Overall goals after completion of the treatment schedule (Table 4) are shown in the last column.

Variable			2010	2017	2018	2019	2020	2021	Percent improvement over 2010 means					Goal after internal P loading
									2017	2018	2019	2020	2021	
Lake	Mean (Jul-Oct)	Mean surface TP (mg/L)	0.074	0.051	0.058	0.035	0.050	0.040	31% reduction	22% reduction	53% reduction	34% reduction	47% reduction	< 0.040
		Mean bottom TP (mg/L)	0.583	0.088	0.246	0.082	0.203	0.120	85% reduction	58% reduction	86% reduction	65% reduction	79% reduction	< 0.050
		Mean bottom SRP (mg/L)	0.467	0.038	0.199	0.02	0.130	0.062	92% reduction	57% reduction	96% reduction	72% reduction	87% reduction	< 0.050
		Mean chlorophyll (ug/L)	47.63	25.17	19.08	24.31	27.88	35.66	47% reduction	60% reduction	49% reduction	41% reduction	25% reduction	< 15
		Mean Secchi transparency (ft)	4.27	6.28	5.41	6.81	5.43	6.19	46% increase	27% increase	59% increase	27% increase	45% increase	12.1
	Early Fall peak (i.e. late August-early October)	Surface TP (mg/L)	0.130	0.081	0.115	0.042	0.074	0.060	38% reduction	11% reduction	68% reduction	43% reduction	54% reduction	NA
		Bottom TP (mg/L)	1.216	0.13	0.543	0.206	0.510	0.223	89% reduction	55% reduction	83% reduction	58% reduction	82% reduction	NA
		Bottom SRP (mg/L)	1.092	0.068	0.468	0.092	0.442	0.156	94% reduction	57% reduction	92% redcution	60% redcution	86% reduction	NA
		Chlorophyll (ug/L)	109.6	42.95	27.63	42.00	64.89	69.70	61% reduction	75% reduction	62% reduction	41% reduction	36% reduction	NA
		Secchi transparency (ft)	2.66	3.61	3.63	3.94	3.12	3.61	36% increase	37% increase	48% increase	17% increase	36% increase	NA
Sediment[1]		Net internal P loading (kg/summer)	3,723	1,150	2,123	-177	1,351	404	69% reduction	42% reduction	100% reduction	64% reduction	89% reduction	< 400
		Net internal P loading (mg/m^2 d)	8.8	3.2	5.6	-0.5	2.8	1.1	64% reduction	36% reduction	100% reduction	68% reduction	88% reduction	< 1.5
		Sediment diffusive P flux (mg/m^2 d)	15.01	11.83	8.34	1.26	4.66	3.72	21% reduction	29% reduction	85% reduction	69% reduction	75% reduction	< 1.5
		Redox-P (mg/g)	0.457	0.298	0.307	0.238	0.415	0.295	35% reduction	33% reduction	48% reduction	9% reduction	36% reduction	< 0.100
		Al-bound P (mg/g)	0.097	0.170	0.331	0.216	0.342	0.308	75% increase	241% increase	123% increase	253% increase	218% increase	NA

[1]Stations 2, 8, 13, 18, and 24

Despite the application of a higher Al dose to a smaller area of sediment, Cedar Lake P mass exhibited modest seasonal increases in 2021 (Fig. 17). For instance, lakewide P mass increased from a low of 670 kg in late June (i.e., during the alum treatment period) to a peak of 1344 kg in mid-August. This peak was still much lower compared to a maximum of > 4,000 kg in 2010. As indicated in James (2014, 2015), summer P mass increases were due almost entirely to internal P loading from anoxic sediment prior to alum treatment. Net internal P loading was substantial in 2010 at 3,723 kg (Table 3). Net internal P loading was 400 in 2021 or 1.1 mg/m^2 d (Table 3). Still, the 2021 net internal P loading rate represented an 88% reduction over the rate estimated for the summer of 2010 (Table 2).

Table 3. Summer net internal phosphorus loading ($P_{net\ int\ load}$) estimates (bold font) for Cedar Lake in 2010 (pretreatment) and 2017-21 (post-treatment).

Summer	Period	$P_{tributary}$	$P_{discharge}$	$P_{retention}$	$P_{lake\ storage}$	$P_{net\ int\ load}$		
	(d)	(kg)	(kg)	(kg)	(kg)	(kg)	(kg/d)	(mg/m^2 d)
2010	97	445	238	207	3,931	**3,723**	**38**	**8.8**
2017	83	349	212	137	1,287	**1,150**	**14**	**3.2**
2018	87	292	128	164	2,288	**2,123**	**24**	**2.8**
2019	85	346	141	205	28	**-77**	**-1**	**0**
2020	112	456	369	87	1,434	**1,351**	**12**	**2.8**
2021[1]	84	293	84	210	614	**404**	**5**	**1.1**

[1] $P_{tributary}$, $P_{discharge}$, and $P_{retention}$ are estimates for the period May through July only due to flow logger vandalism.

The pattern of seasonal P mass increase in the hypolimnion was still improved in 2021, coincident with the alum application, versus 2010 (Fig. 18). In 2010 (before Al application), the anoxic hypolimnion accounted for most of the seasonal P mass increase (Fig. 18). By comparison, hypolimnetic P mass accumulation was lower in 2021, indicating overall suppression of net internal P loading from anoxic sediment (Fig. 18).

Changes in sediment chemistry and anaerobic diffusive phosphorus flux

Laboratory-derived anaerobic diffusive P fluxes declined in September 2021 at both the central

WQ2 station and stations located along the north-south transect (i.e., stations 2, 8, 13, 18, and 24) after the June 2021 alum application (Fig. 19). The mean anaerobic diffusive P flux along the transect stations 2, 8, 12, 18, and 24 was 3.7 mg/m^2 d in 2021, representing a 75% decline over the pretreatment rate of 8.8 mg/m^2 d (Table 2). This decline corroborated with similar patterns in lake P mass accumulation (Fig. 20).

Spatially throughout lake depths > 20 ft, anaerobic diffusive P fluxes were lower by 40% to 96% in 2021 versus pretreatment fluxes measured prior to the first alum treatment in June 2017 (Fig. 21). Comparison of mean anaerobic diffusive P flux in the 2021 alum treatment zone (depths > 25 ft) versus the mean in the 20-25-ft depth contour are shown in Figure 22. The 20-ft to 25-ft depth contour zone was treated with alum in 2017 and 2019 but not in 2021. The > 25-ft depth contour was treated with alum in 2017, 2019, and 2021. Although not statistically significant, the mean anaerobic diffusive P flux (n = 8) was lower in the recently treated zone (> 25 ft) at 3.6 mg/m^2 d compared to the mean 5.1 mg/m^2 d (n = 7) in the 20-ft to 25-ft depth contour zone (Fig. 22c). Improvement over pretreatment P fluxes were also greater in the recently treated > 25-ft depth contour at 79% versus fluxes in the 20-ft to 25-ft depth contour at 59%. (Fig. 22d).

Overall, total aluminum (Al) concentrations in the surface sediment have increased in most areas of the lake bottom in conjunction with the 3 alum applications (Fig. 23). Because the 3rd alum application was targeted for sediments located at depths > 25 ft in 2021, the mean total Al concentration was greatest in this depth zone versus the mean within the 20-25 ft depth zone (Fig. 24).

One difficulty has been estimating the area-based Al concentration (i.e., g/m^2) from spatially-distributed surface sediment slices because the thickness of the added alum layer in the sediment section is not precisely known and probably less than the thickness of the sediment slice (Fig. 25). Thus, the native sediment Al concentration must be subtracted out from the calculation in order to estimate the added alum. I assumed the added alum layer thickness was ~ 5 cm to calculate the area-based concentration. However, in the future sediment vertical profiles (i.e., see Fig. 29) will be needed to construct a more accurate estimate of the added alum concentration.

Under the above assumptions, the estimated area-based Al concentrations were generally highest at depths > 25 ft and lower in the 20-25-ft depth zone (Fig. 25). Comparisons along the central longitudinal transect of the lake suggested that added alum concentrations in the center and southern portions of the deep sediment (> 25 ft) were below but approached the target 100 g/m^2 as of 2021 (Fig. 26 & 27). The sediments located in the northern portions of this treatment zone exhibited lower area-based Al concentrations. The area-based Al concentration at Station CL 24, located within the 20-25-ft depth zone, was similar to the target added alum concentration of ~ 42 g/m^2. Overall, the mean area-based Al concentration in the > 25 ft depth zone was ~ 61 g/m^2 and ~ 43 g/m^2 in the 20-25-ft depth zone (Fig. 24). But caution needs to be used in interpreting these results. More detailed vertical sediment concentration profiles will be collected in 2022 for more accurate determinations of area-based Al concentration.

Spatial variations in redox-P and aluminum-bound P in the upper 10-cm sediment layer are shown in Fig. 28 for stations located in the recently alum-treated zone (i.e., depths > 25 ft) and the 20-ft to 25-ft depth zone. Redox P concentrations have declined in both zones as of 2021. Mean redox P was slightly higher in the > 25-ft depth contour zone versus the mean in the 20-ft to 25-ft depth contour zone in 2021 (Fig. 22a). Aluminum-bound P exhibited a trend of increasing concentration at all stations located in the > 25-ft depth contour as of 2021 versus the pretreatment year 2017, suggesting considerable P binding onto the alum floc (Fig. 28). In contrast, concentrations have not changed much in 2021 compared to pretreatment 2017 concentrations for Al-treated sediments located between the 20-ft to 25-ft contour (Fig. 28). Overall, mean aluminum-bound P concentrations in the upper 10-cm sediment section were much greater in the > 25-ft depth contour zone versus the 20-ft to 25-ft depth contour zone as of 2021 (Fig. 22d). This pattern could be attributed to lower Al concentrations in the 20-ft to 25-ft depth contour.

At station WQ 2, vertical variations in sediment moisture content and density reflected the positioning of the Al floc newly-applied in 2021 at the sediment surface (Fig. 29). Sediment moisture content was higher, while sediment density was lower, in the upper 2-cm layer in the core collected in September 2021 versus the core collected immediately prior to the initial alum application in June 2017 (Fig. 29). The Al floc is typically very flocculent with densities only

slightly > than that of water when first applied, resulting in deposition primarily on top of the sediment-water interface (James 2017). Redox P concentrations have declined in the 0-cm to 4-cm sediment layer relative to much higher concentrations in that layer in 2017, suggesting binding of P onto the Al floc. In addition, aluminum-bound P concentrations have increase in the 0-cm to 4-cm layer as well as in the new Al floc as a result of P binding.

Recommendations

The 4th alum application can be scheduled for as early as 2023. However, Al dosage and treatment areas for this application need to be assessed based on findings from the monitoring study to be conducted in 2022. The 2022 findings will be critical in answering the following questions:

1. Do we continue to treat only the sediment contained within the > 25-ft depth contour with the higher Al dose,
2. Or should we go back to the original treatment scenario where sediments within the 20-ft to 25-ft depth contour are treated with a 20 g/m^2 dose while sediments within the > 25-ft depth contour are treated with a 26 g/m^2 dose.

References

APHA (American Public Health Association). 2011. Standard Methods for the Examination of Water and Wastewater. 22th ed. American Public Health Association, American Water Works Association, Water Environment Federation.

Avnimelech Y, Ritvo G, Meijer LE, Kochba M. 2001. Water content, organic carbon and dry bulk density in flooded sediments. Aquacult Eng 25:25-33.

de Vicente I, Huang P, Andersen FØ, Jensen HS. 2008. Phosphate adsorption by fresh and aged aluminum hydroxide. Consequences for lake restoration. Environ Sci Technol 42:6650-6655.

Håkanson L, Jansson M. 2002. Principles of lake sedimentology. The Blackburn Press, Caldwell, NJ USA.

Hjieltjes AH, Lijklema L. 1980. Fractionation of inorganic phosphorus in calcareous sediments. J Environ Qual 8: 130-132.

James WF. 2012. Limnological and aquatic macrophyte biomass characteristics in Half Moon Lake, Eau Claire, Wisconsin, 2012: Interim letter report. University of Wisconsin – Stout, Sustainability Sciences Institute – Discovery Center, Menomonie, WI.

James WF. 2014. Phosphorus budget and management strategies for Cedar Lake, WI. University of Wisconsin – Stout, Sustainability Sciences Institute – Discovery Center, Menomonie, WI.

James WF. 2017. Phosphorus binding dynamics in the aluminum floc layer of Half Moon Lake, Wisconsin. Lake Reserv Manage 33:130-142.

James WF, PW Sorge, PJ Garrison. 2015. Managing internal phosphorus loading in a weakly stratified eutrophic lake. Lake Reserv Manage 31:292-305.

Mortimer CH. 1971. Chemical exchanges between sediments and water in the Great Lakes – Speculations on probable regulatory mechanisms. Limnol Oceanogr 16:387-404.

Nürnberg GK. 1988. Prediction of phosphorus release rates from total and reductant-soluble phosphorus in anoxic lake sediments. Can J Fish Aquat Sci 45:453-462.

Nürnberg GK. 2009. Assessing internal phosphorus load – Problems to be solved. Lake Reserv Manage 25:419-432.

Pilgrim KM, Huser BJ, Brezonik PL. 2007. A method for comparative evaluation of whole-lake and inflow alum treatment. Wat Res. 41:1215-1224.

Psenner R, Puckso R. 1988. Phosphorus fractionation: Advantages and limits of the method for the study of sediment P origins and interactions. Arch Hydrobiol Biel Erg Limnol 30:43-59.

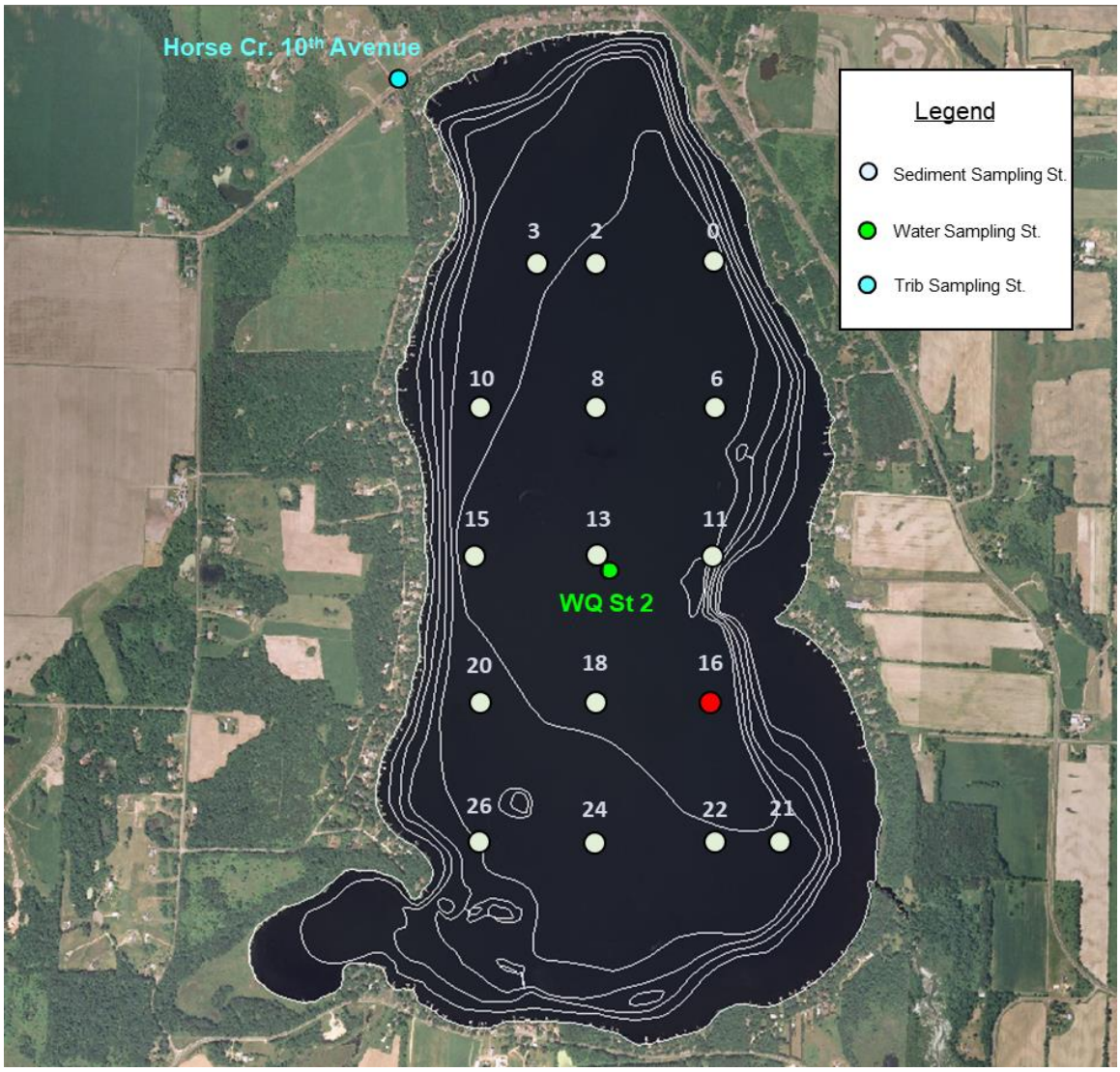

Figure 1. Sediment and water sampling stations in 2021. There was not enough sediment for analysis from the cores collected at Station 16.

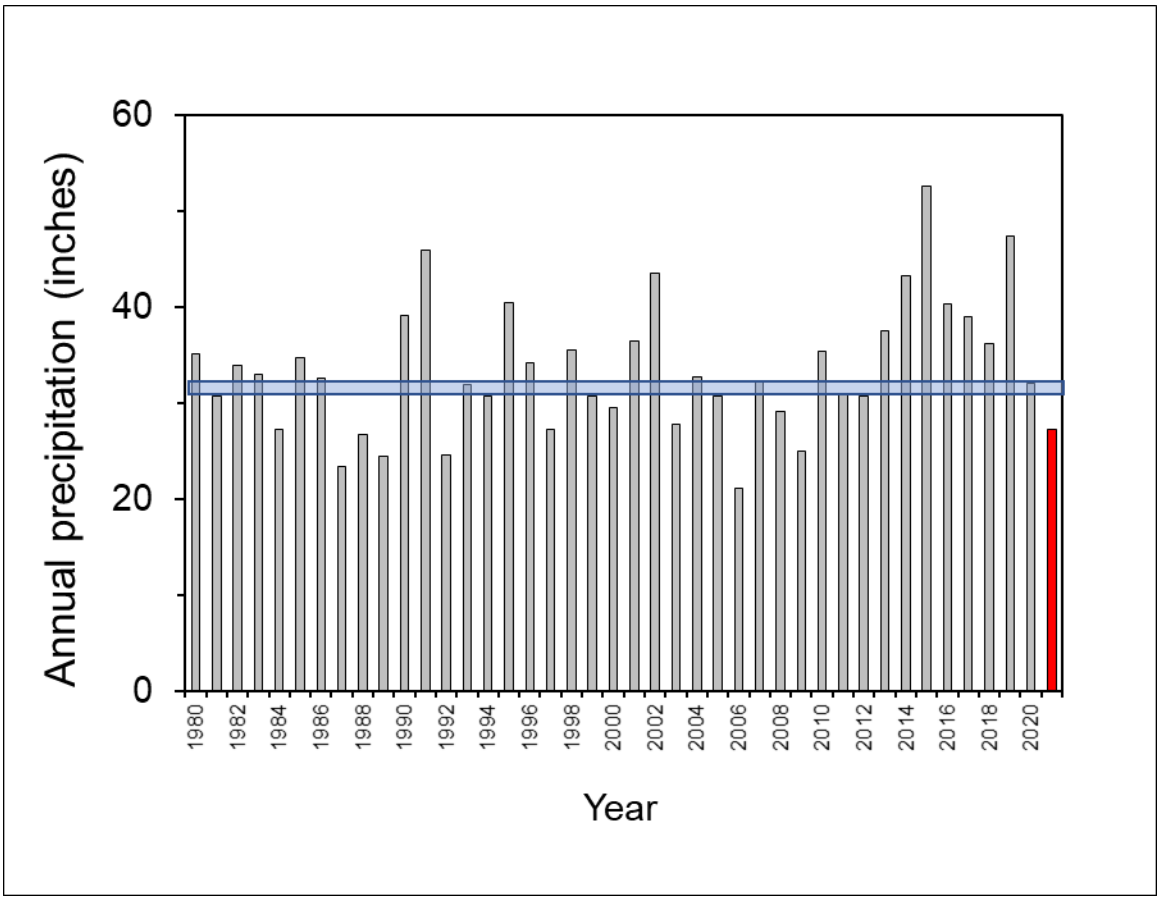

Figure 2. Variations in annual precipitation at Amery, WI. Blue horizontal line represents the average. The year 2021 is highlighted in red.

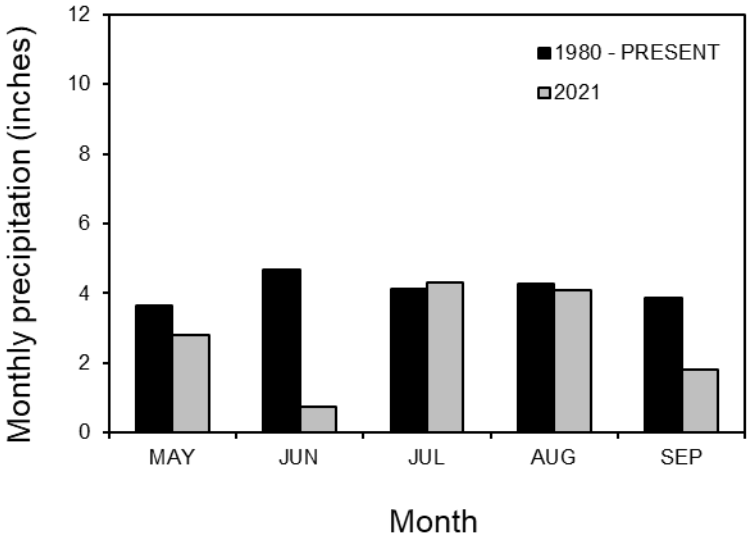

Figure 3. A comparison of average monthly precipitation.

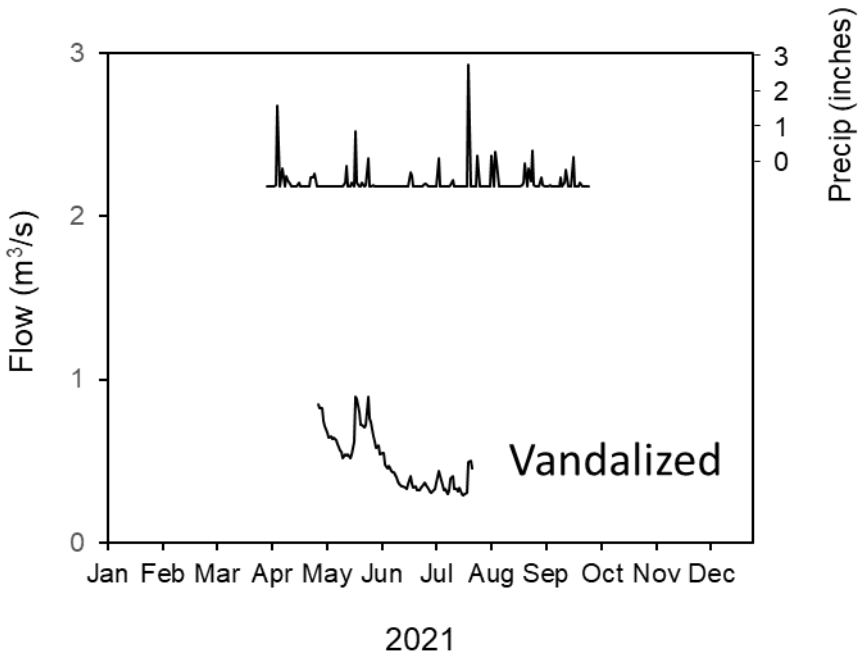

Figure 4. Seasonal variations in daily precipitation at Amery, WI, and flow for Horse Creek at 10th Ave. The flow logger was vandalized in late July.

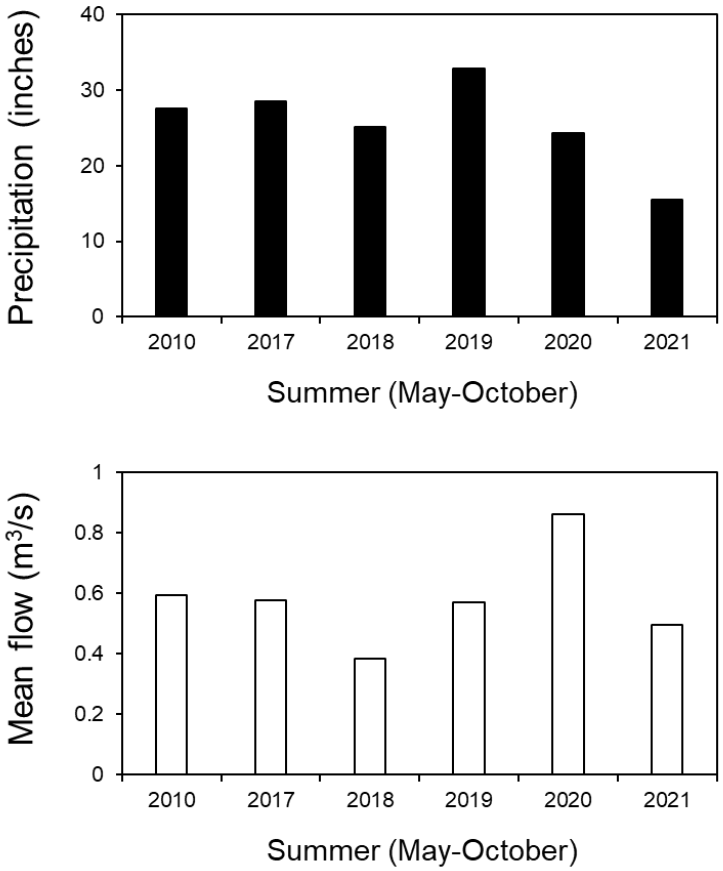

Figure 5. A comparison of summer (May-October) precipitation (upper panel) and mean Horse Creek flow (lower panel). The summer of 2010 was a pretreatment year. Alum was applied to the lake in late June 2017, 2019, and 2021.

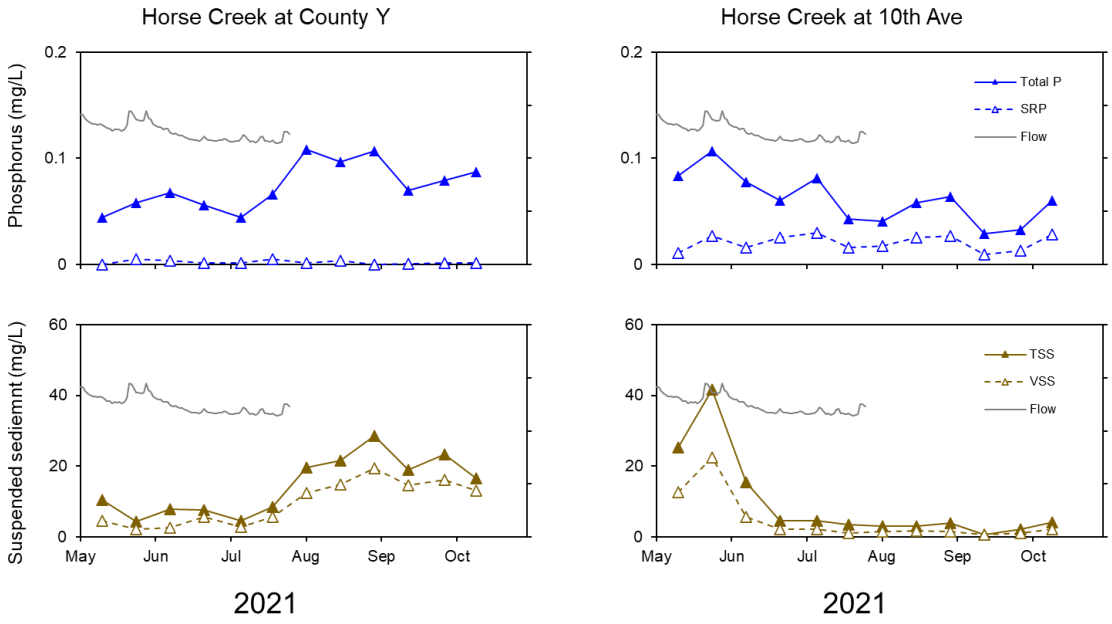

Figure 6. Seasonal variations in total phosphorus (P) and soluble reactive P (SRP) concentration at Horse Creek County Y (i.e., below Horse Lake) and 10th Ave (i.e., mouth to Cedar Lake).

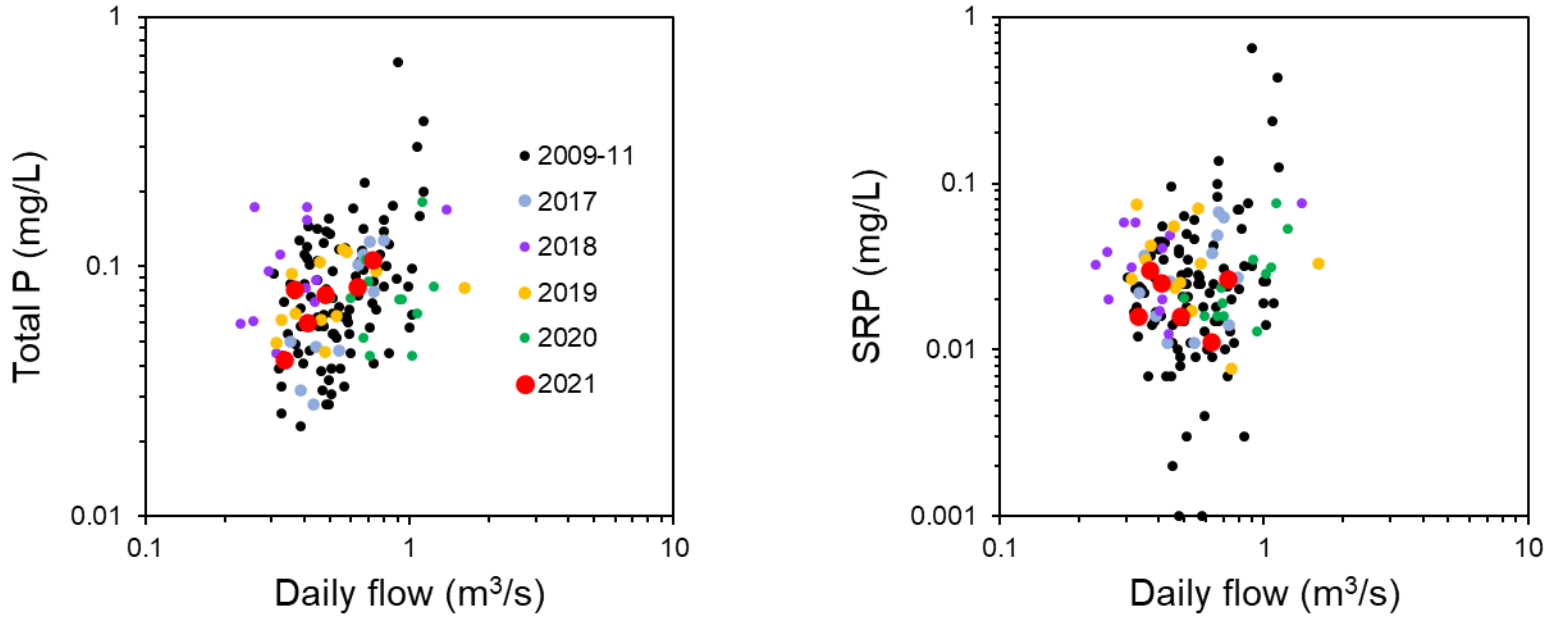

Figure 7. Phosphorus (P) concentration versus daily flow at Horse Creek.

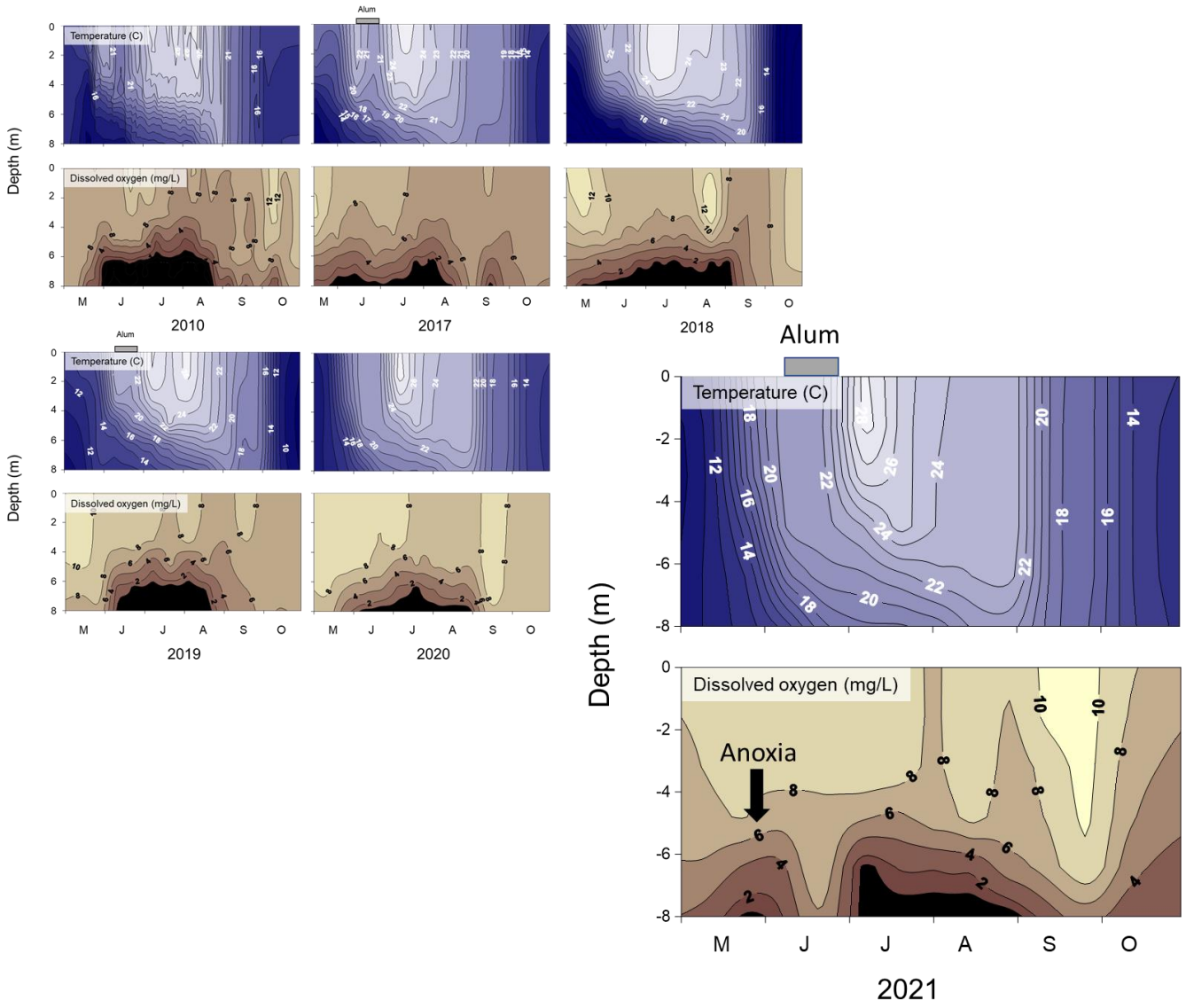

Figure 8. Seasonal and vertical variations in temperature (upper panels) and dissolved oxygen (lower panels) in 2010 (pre-treatment) and 2017-2021 (after alum treatment). Alum was applied in June 2017, 2019, and 2021.

Figure 9. Seasonal variations in bottom (i.e., ~ 0.25 m above the sediment-water interface) total phosphorus (P), and bottom soluble reactive P (SRP) during a pretreatment year (2010) and the post-alum treatment years 2017-21. Alum was applied in June 2017, 2019, and 2021.

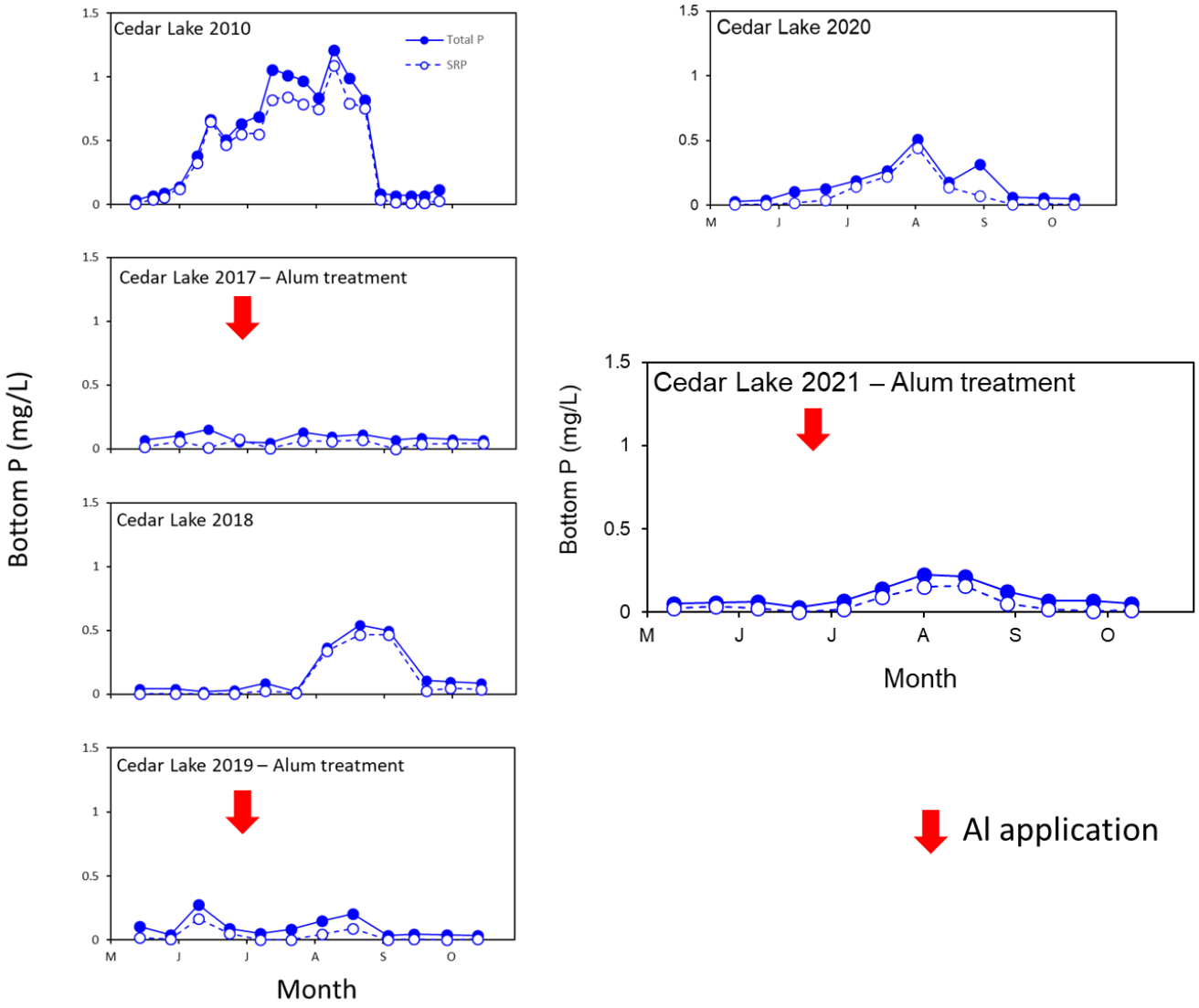

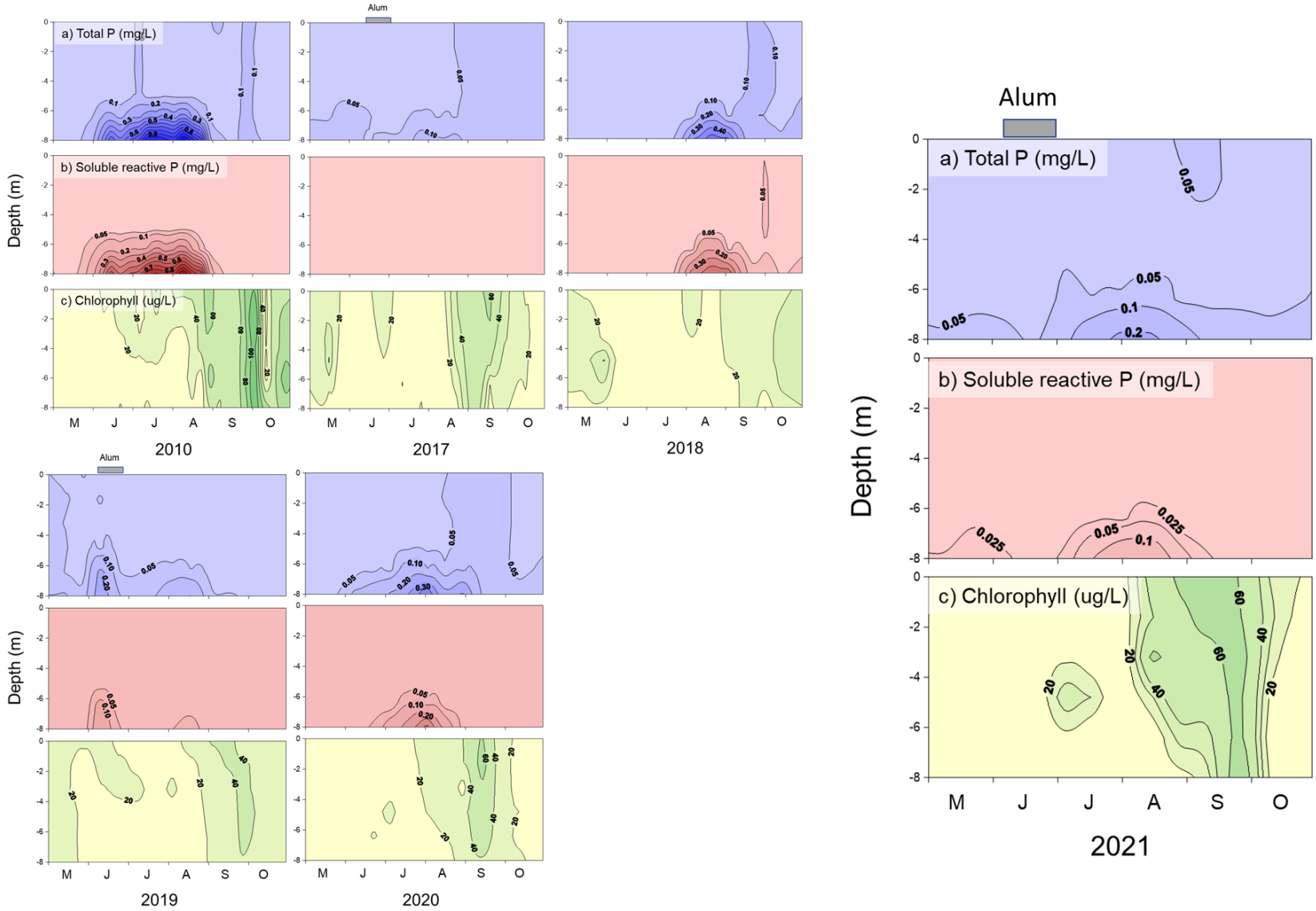

Figure 10. Seasonal and vertical variations in a) total phosphorus (P), b) soluble reactive P, and c) chlorophyll in 2010 (pretreatment) versus 2017-21 (post-treatment). Alum was applied in June 2017, 2019, and 2021.

Figure 11. Seasonal variations in surface total phosphorus (P), during a pretreatment year (2010) and the post-alum treatment years 2017-21. Alum was applied in June 2017, 2019, and 2021.

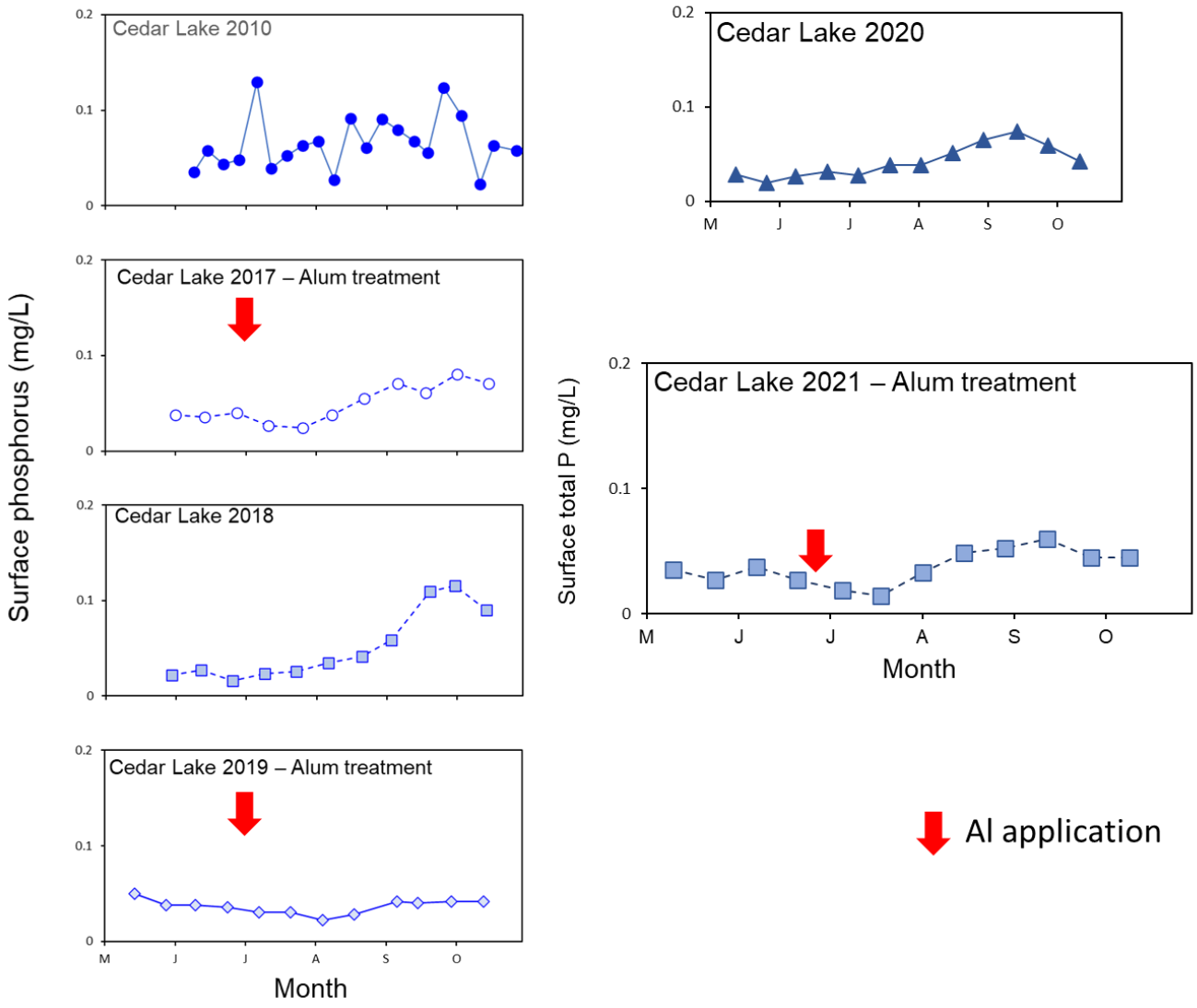

Figure 12. Seasonal variations in surface chlorophyll during a pretreatment year (2010) and the post-alum treatment years 2017-21. Alum was applied in June 2017, 2019, and 2021.

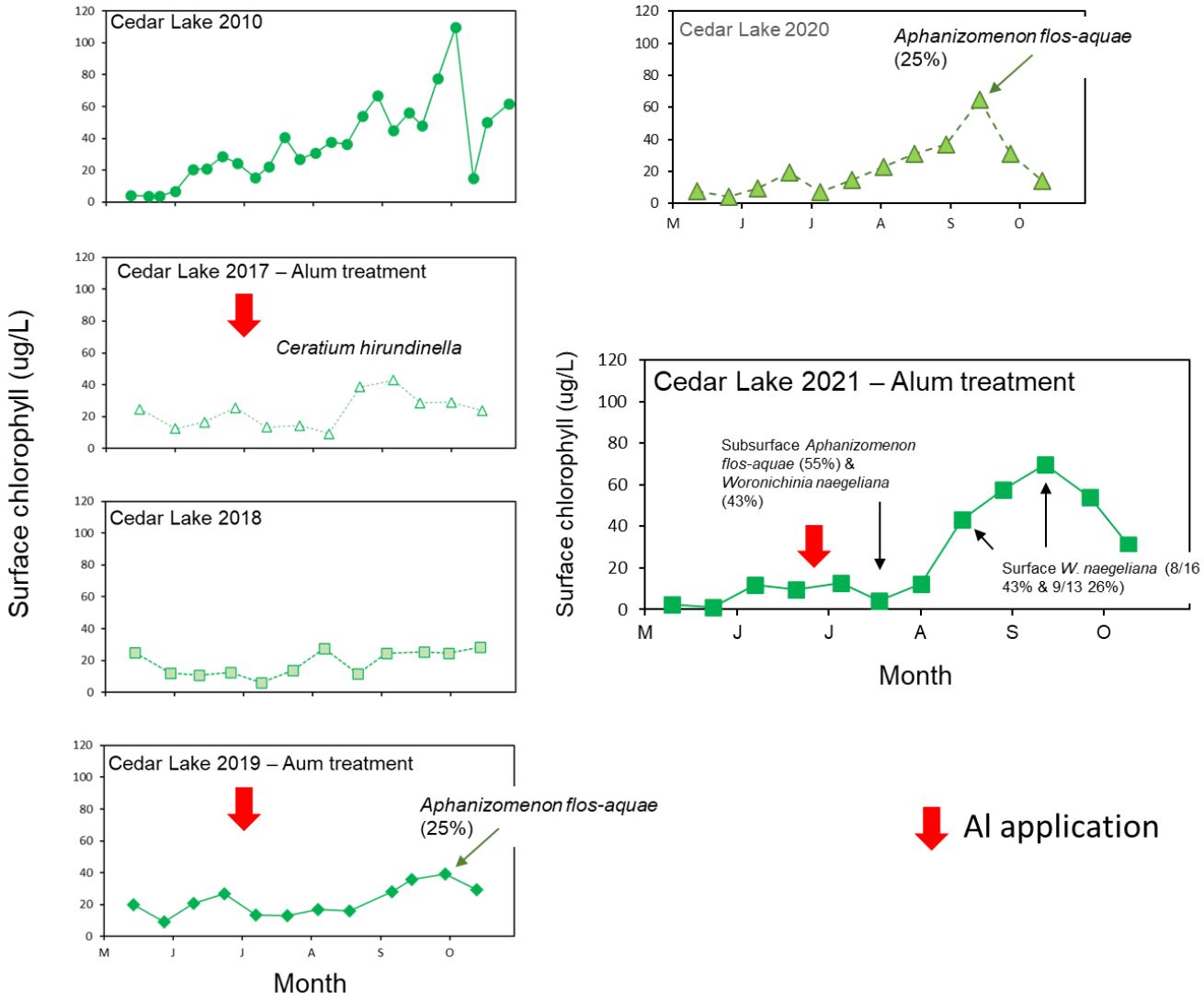

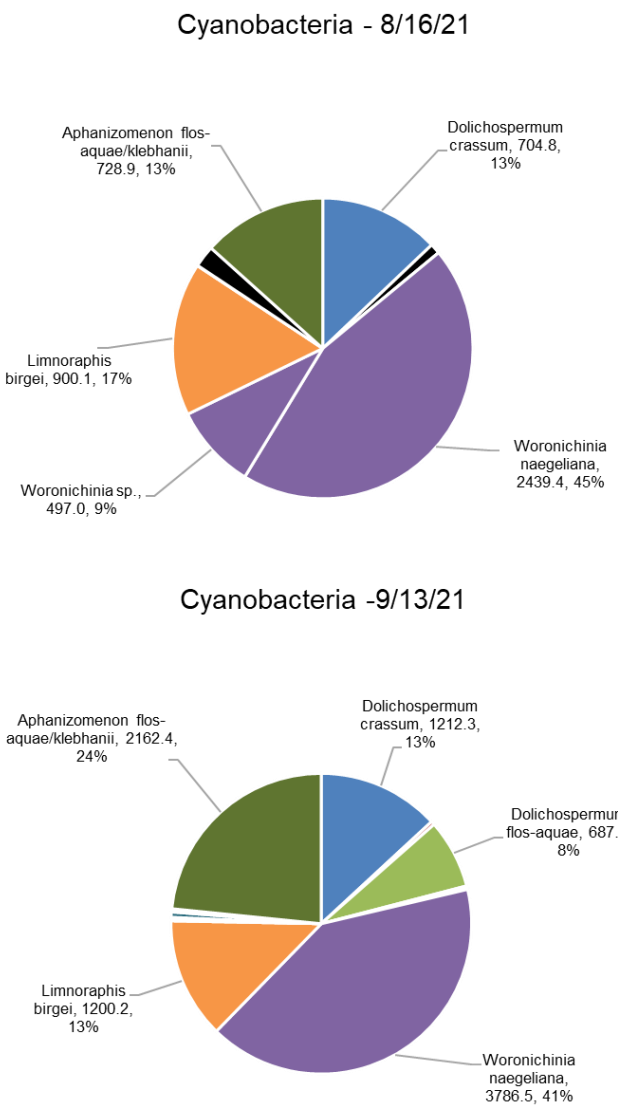

Figure 13. Major cyanobacteria genera biomass in the upper 2-m on 16 August 2021 and 13 September 2021.

Figure 14. Seasonal variations in Secchi transparency during a pretreatment year (2010) and the post-alum treatment years 2017-21. Alum was applied in June 2017, 2019, and 2021.

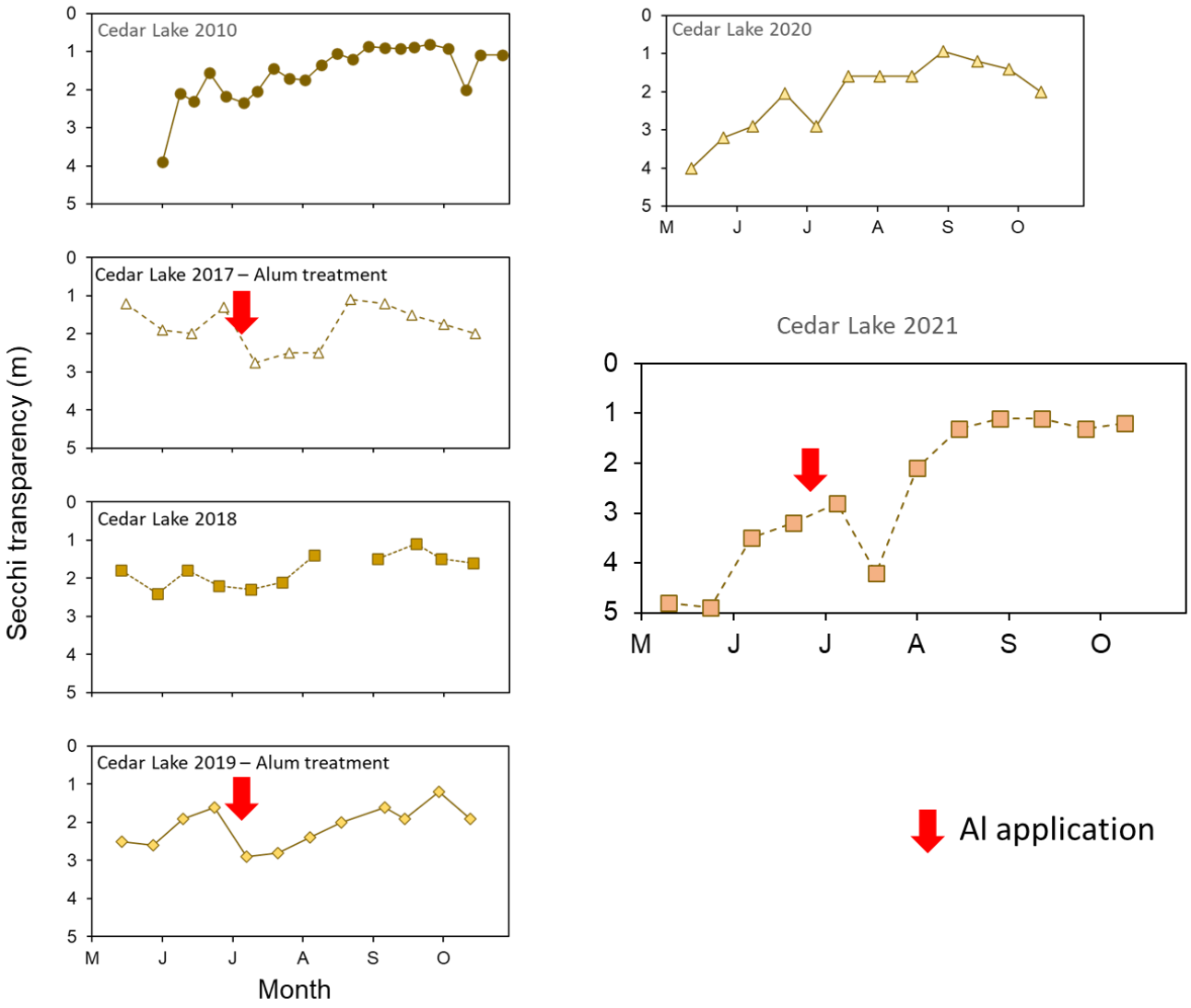

Figure 15. Relationships between Secchi transparency and chlorophyll (upper panel) and total phosphorus (P) versus chlorophyll (lower panel) during the summer 2017-2021.

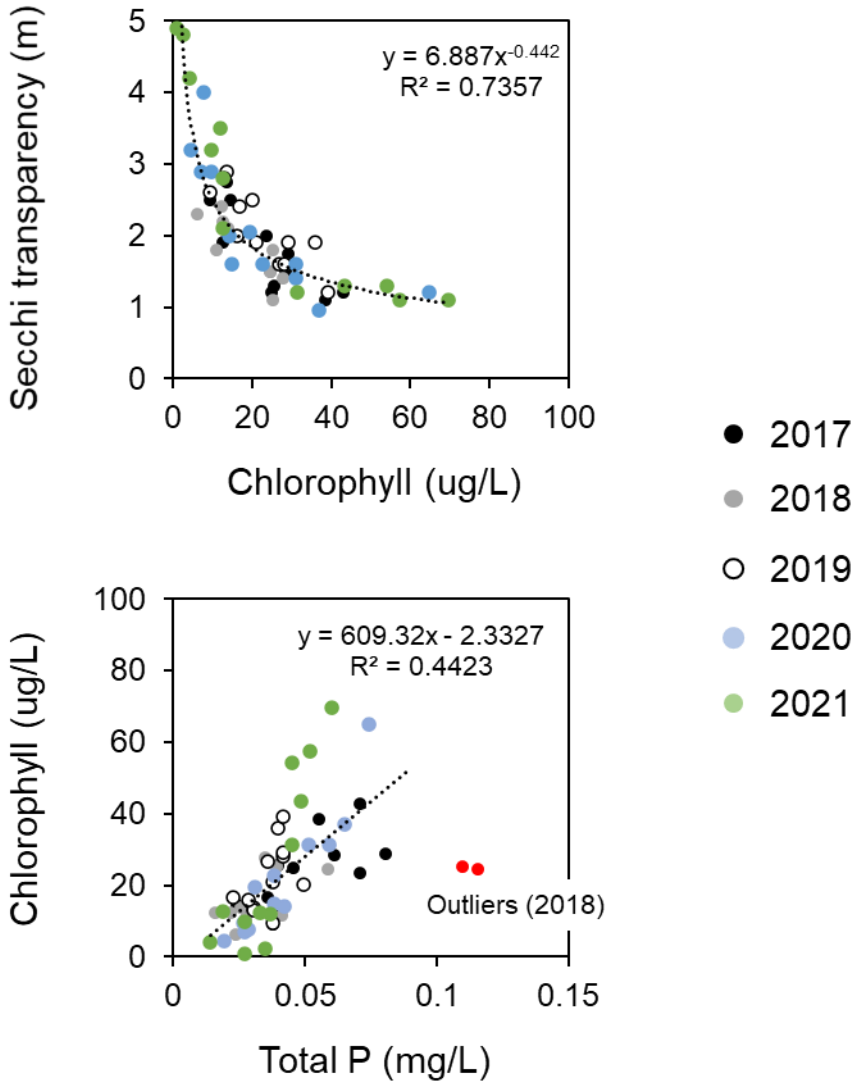

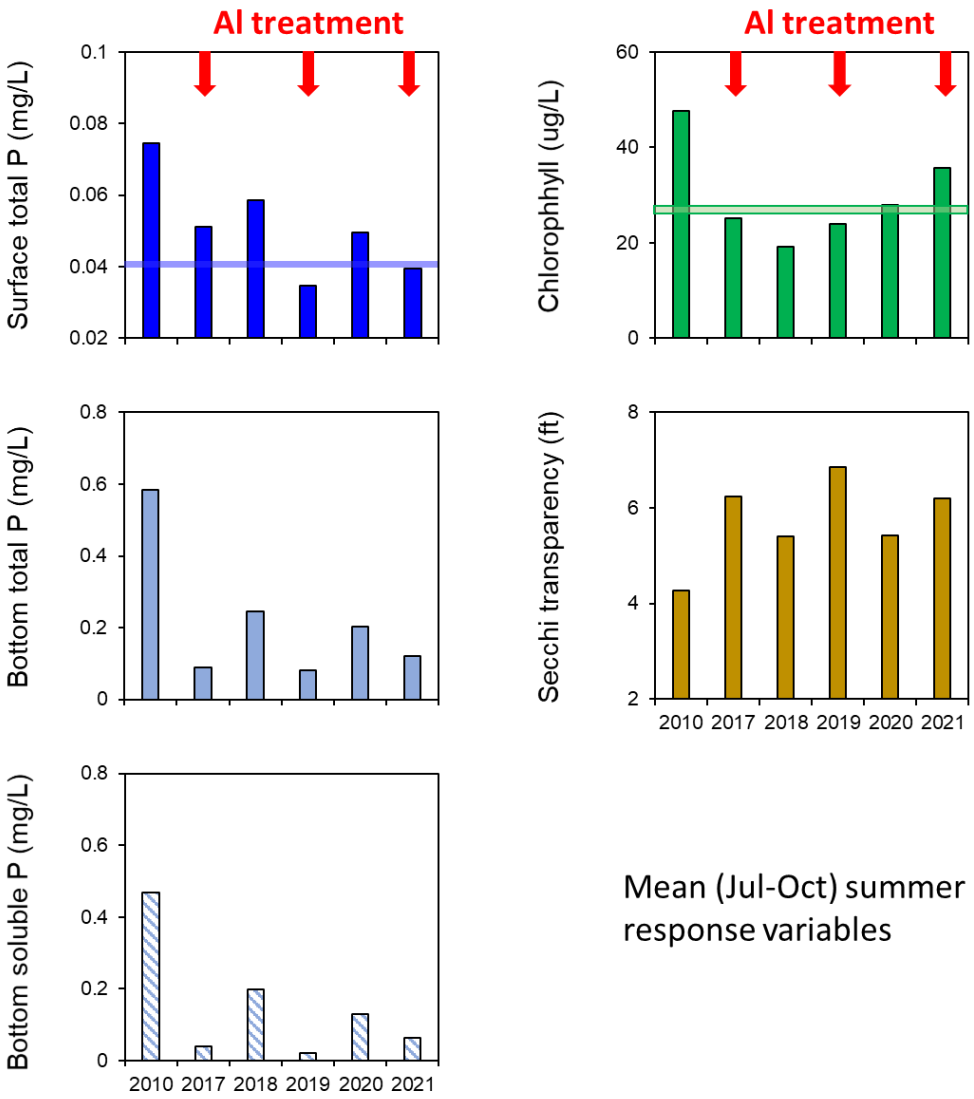

Figure 16. A comparison of mean summer (July-early October) summer concentrations of surface and bottom total phosphorus (P) and soluble reactive P (SRP), chlorophyll and Secchi transparency during a pretreatment year (2010) and the post-treatment years 2017-21. Alum was applied in June 2017, 2019, and 2021.

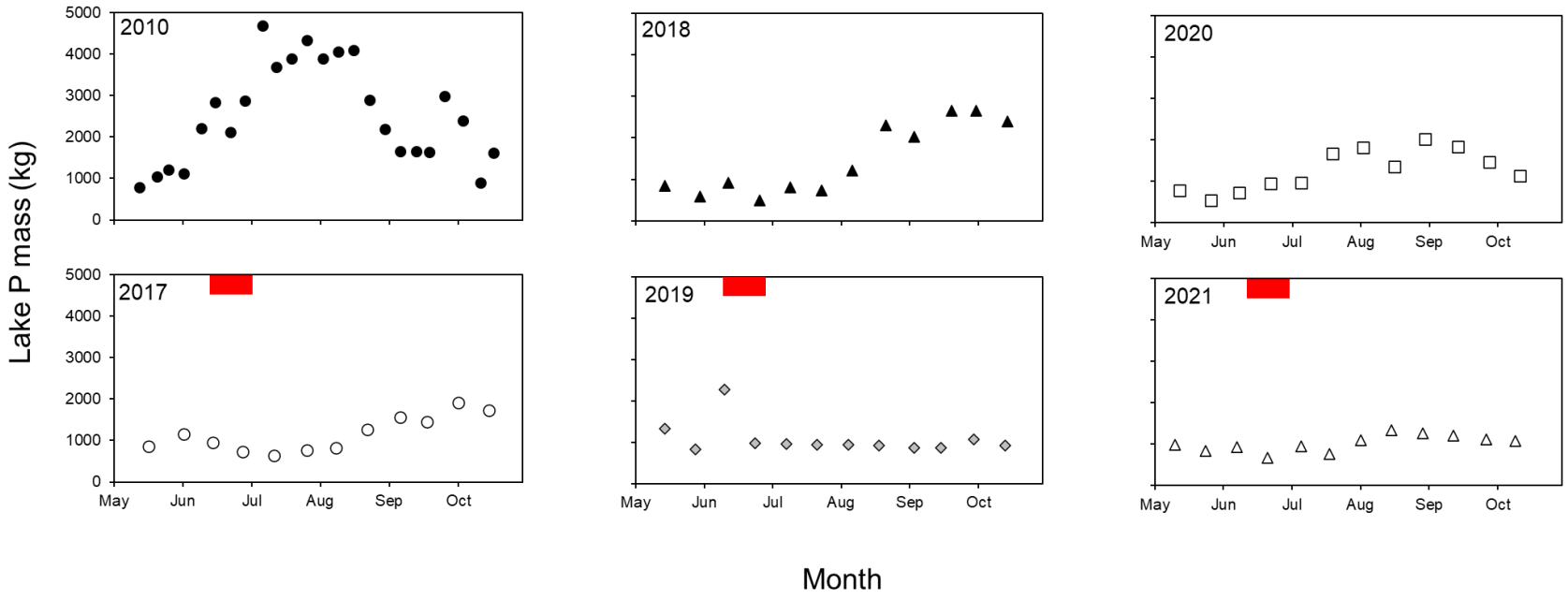

Figure 17. Seasonal variations in total phosphorus (P) mass during a pretreatment year (2010) and the post-treatment years 2017-21. Alum was applied in June 2017, 2019, and 2021.

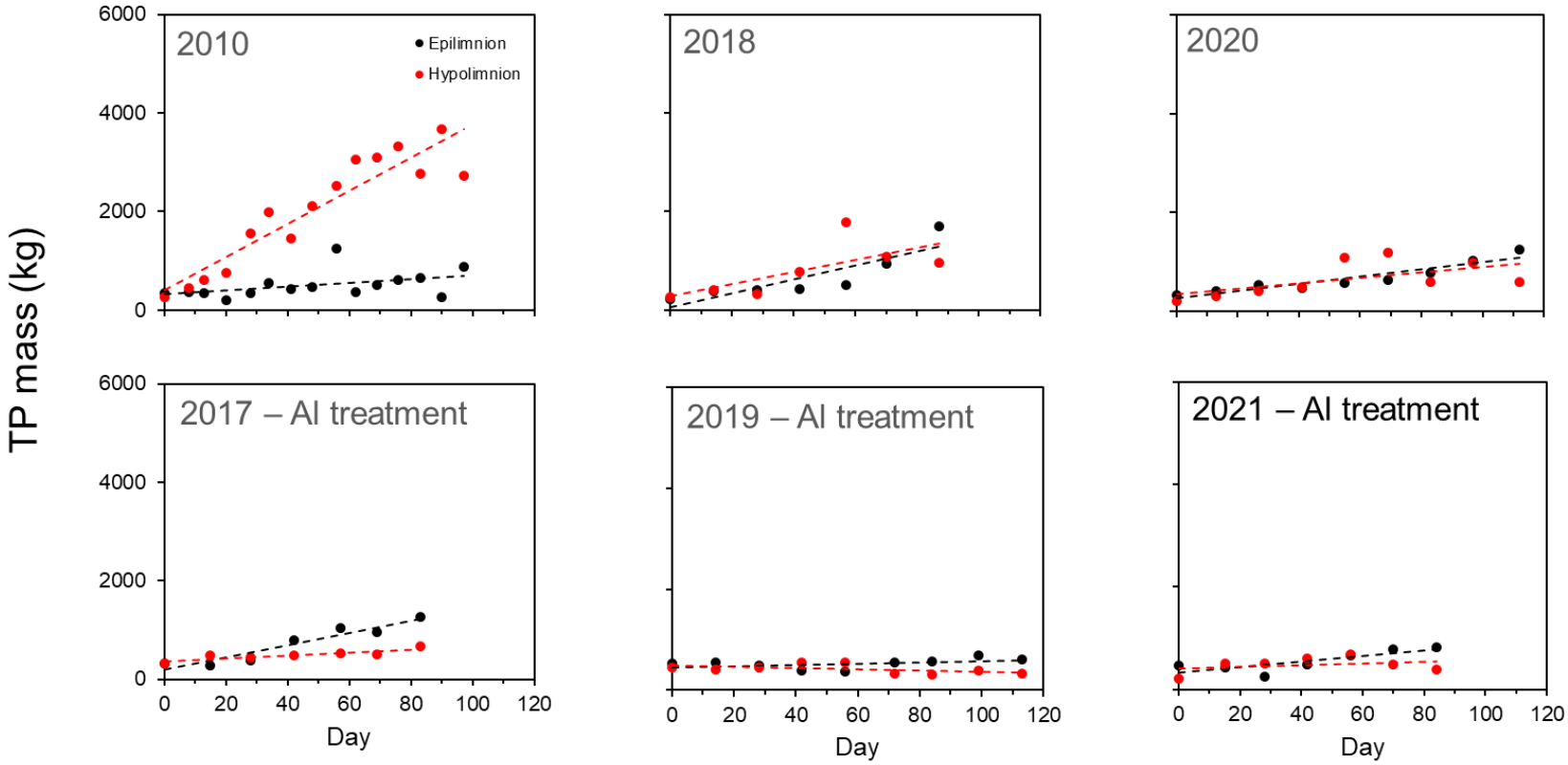

Figure 18. Seasonal variations in total phosphorus (P) mass in the epilimnion (i.e., 0-4 m) and hypolimnion (> 4 m) during a pretreatment year (2010) and the post-treatment years 2017-21. Alum was applied in June 2017, 2019, 2021.

Figure 19. Variations in anaerobic diffusive phosphorus (P) flux (mg/m^2 d) before (June 2010 and 2017) and after the 1st through 3rd alum application. WQ-2 = the centrally-located water quality sampling station. Spatial = the means from stations 3, 8, 13, 18, and 24 (see Fig. 1)

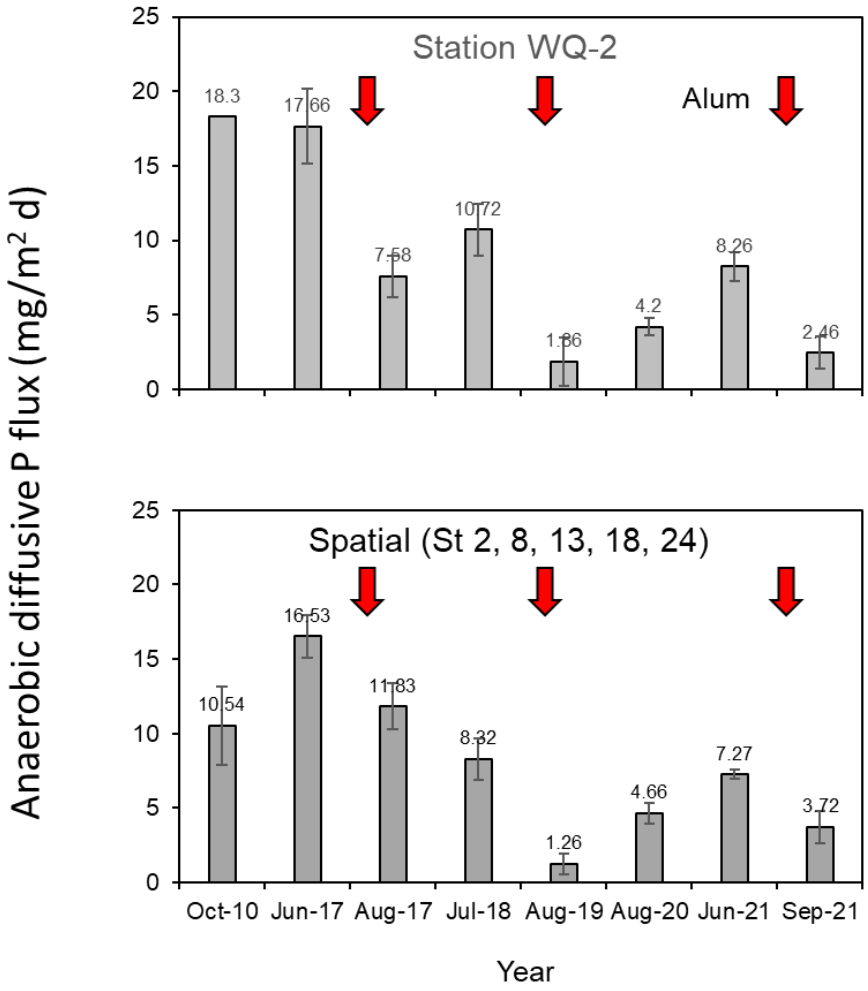

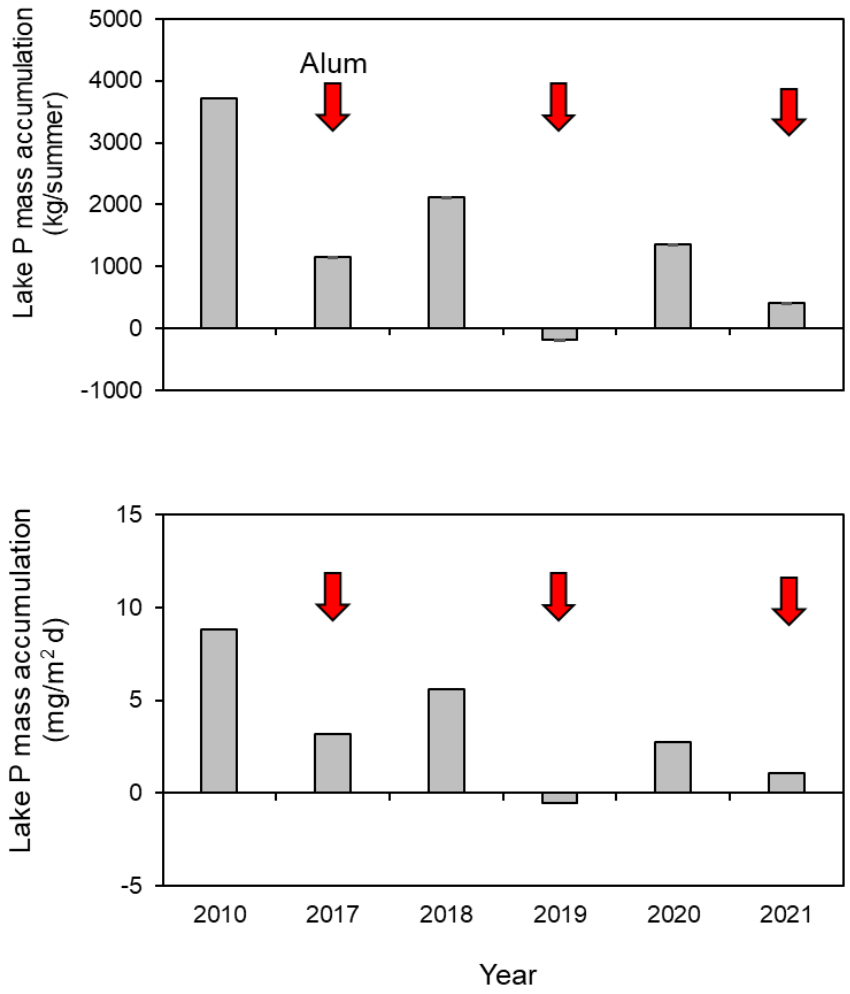

Figure 20. Variations in lake phosphorus (P) mass accumulation before (June 2010 and 2017) and after 1st through 3rd alum application.

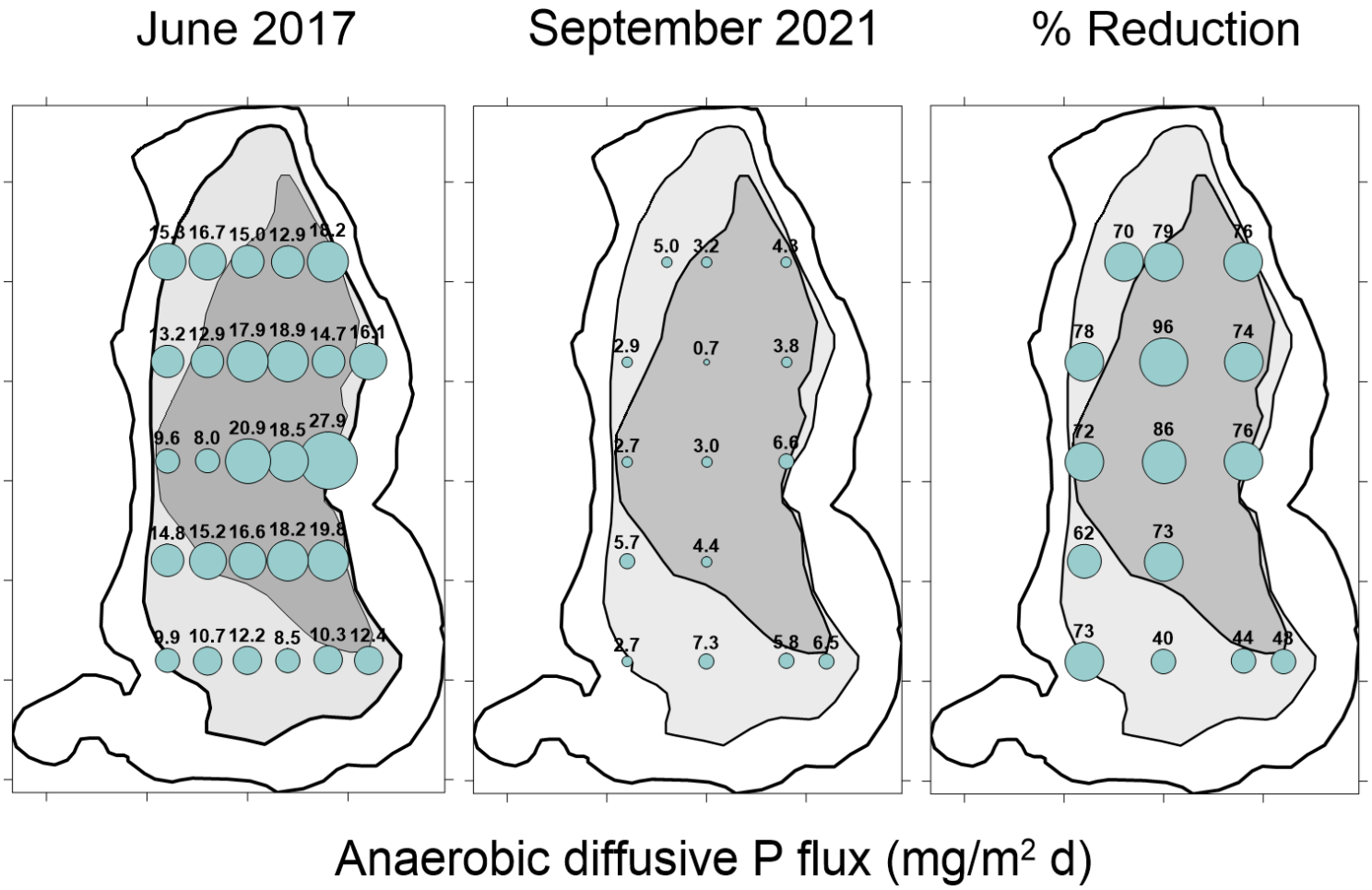

Figure 21. A comparison of spatial variations in laboratory-derived anaerobic diffusive P flux from sediment immediately before the initial alum treatment in 2017 (left), after the 3rd alum application in 2021 (center), and percent improvement or reduction as of 2021 (right).

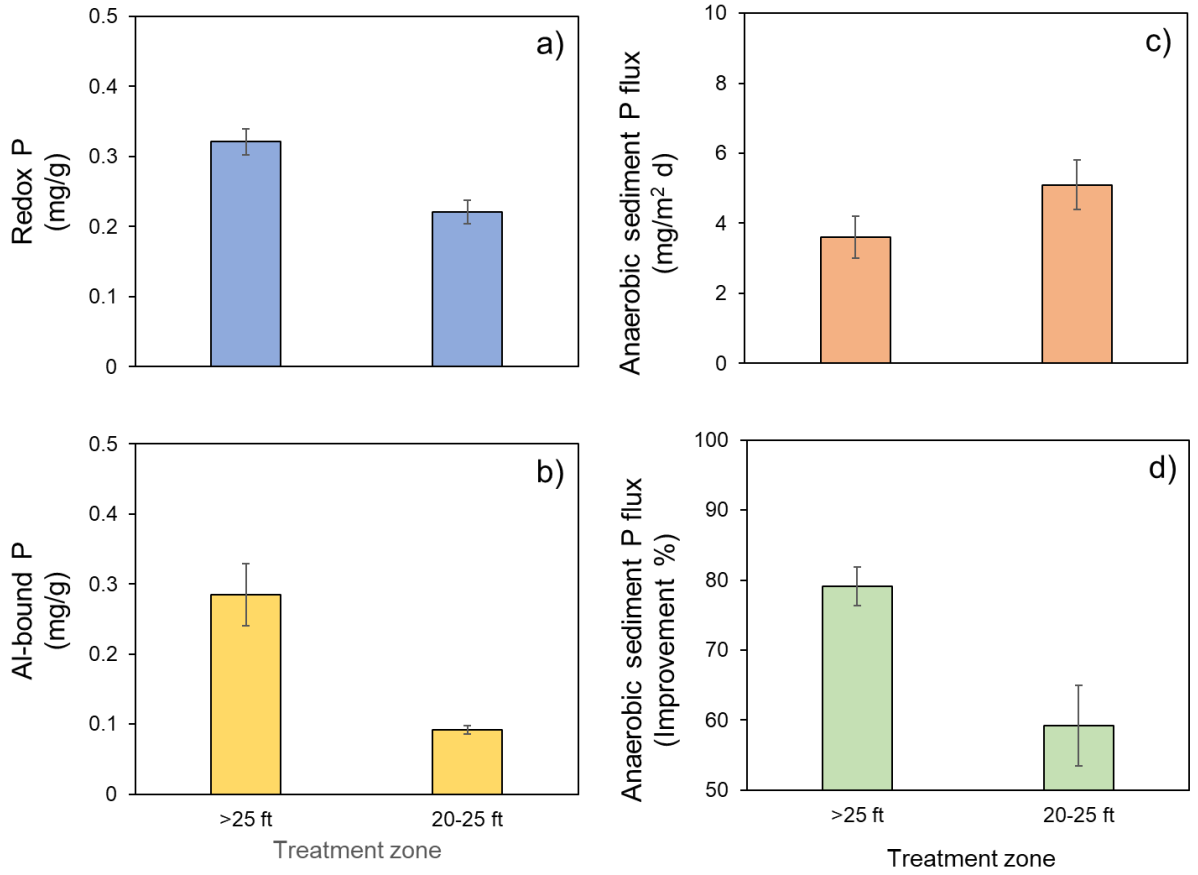

Figure 22. Mean redox P (a), aluminum-bound P (b), laboratory-derived anaerobic diffusive P flux (c), and anaerobic P flux percent improvement or reduction in 2021 (d) in the > 25-ft depth contour treatment zone (n=8) versus the 20-ft to 25-ft depth contour treatment zone (n=7).

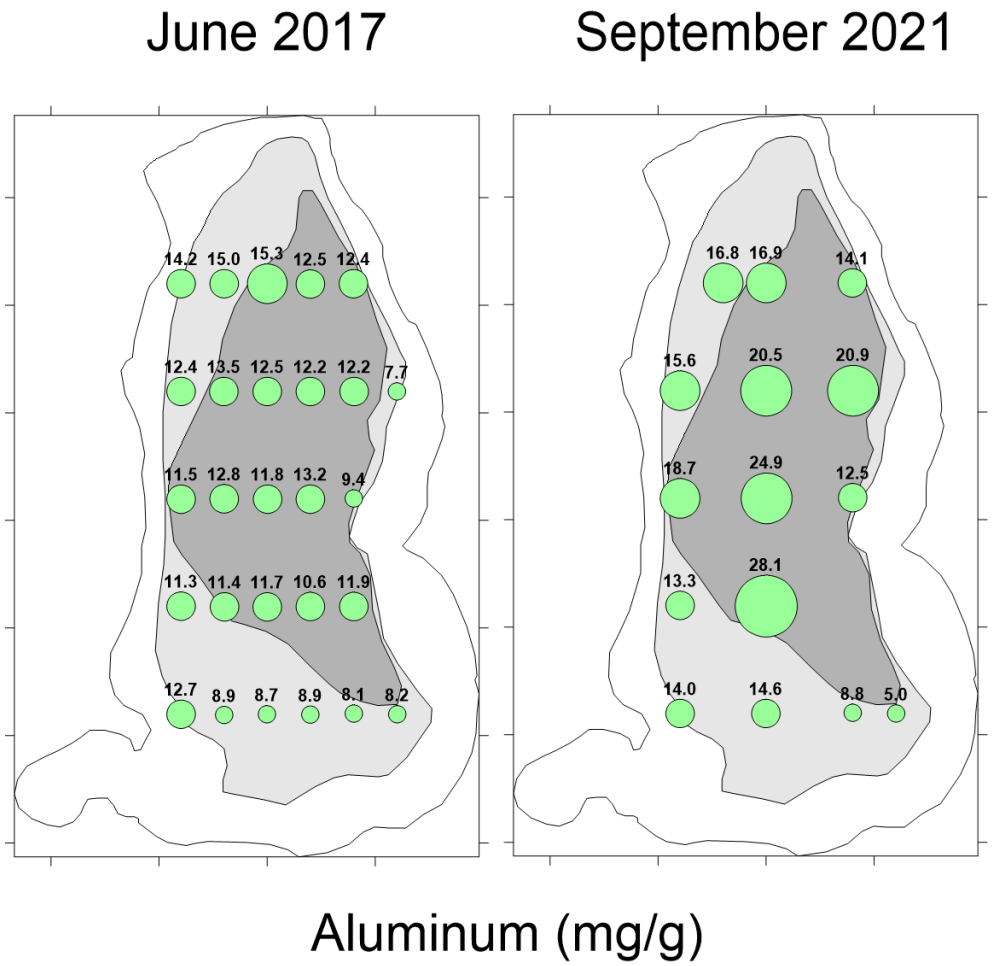

Figure 23. A comparison of spatial variations in sediment total aluminum in the upper 10-cm sediment section immediately before the initial alum treatment in 2017 (left) and after the 3rd alum application in 2021 (right).

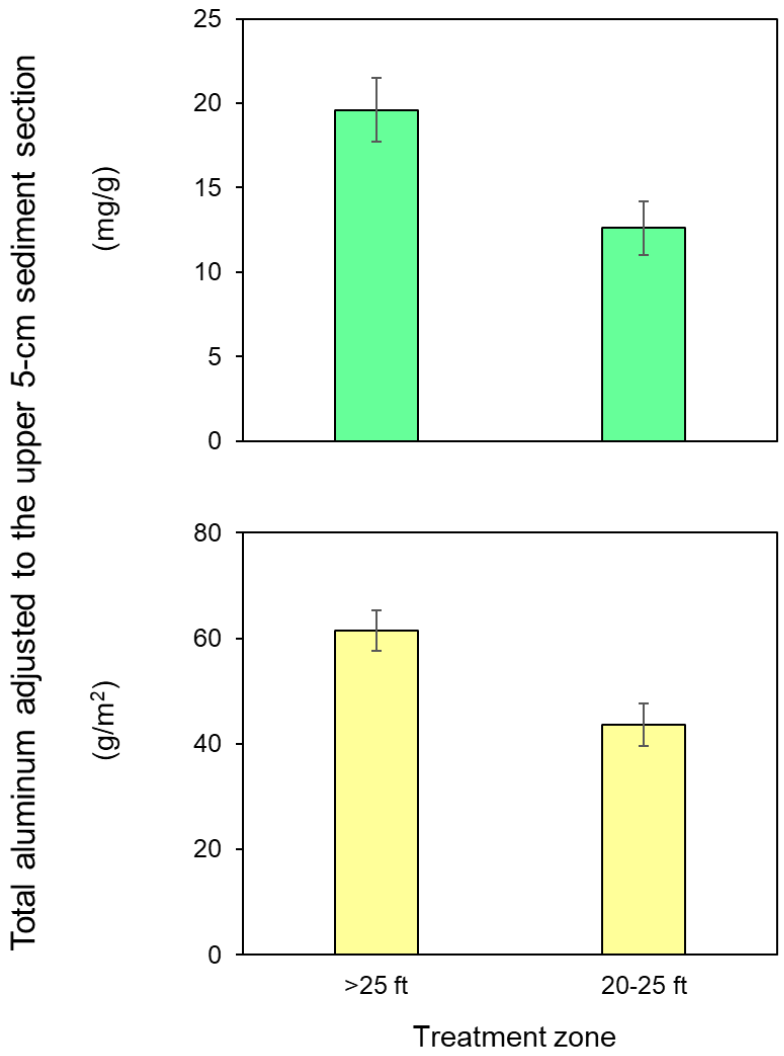

Figure 24. Mean estimated aluminum concentration in the > 25-ft depth contour treatment zone (n=8) versus the 20-ft to 25-ft depth contour treatment zone (n=7). The area-based Al concentration was estimated based on the assumption that the Al floc layer was 5-cm in thickness and occupied the upper region to the sediment core slice.

Figure 25. Spatial variations in the estimated area-based sediment total aluminum concentration (see Figure 1) after the 3rd alum application in 2021. The area-based Al concentration was estimated based on the assumption that the Al floc layer was 5-cm in thickness and occupied the upper region to the sediment core slice. Background represents the Al concentration of the native sediment before the initiation of alum treatment

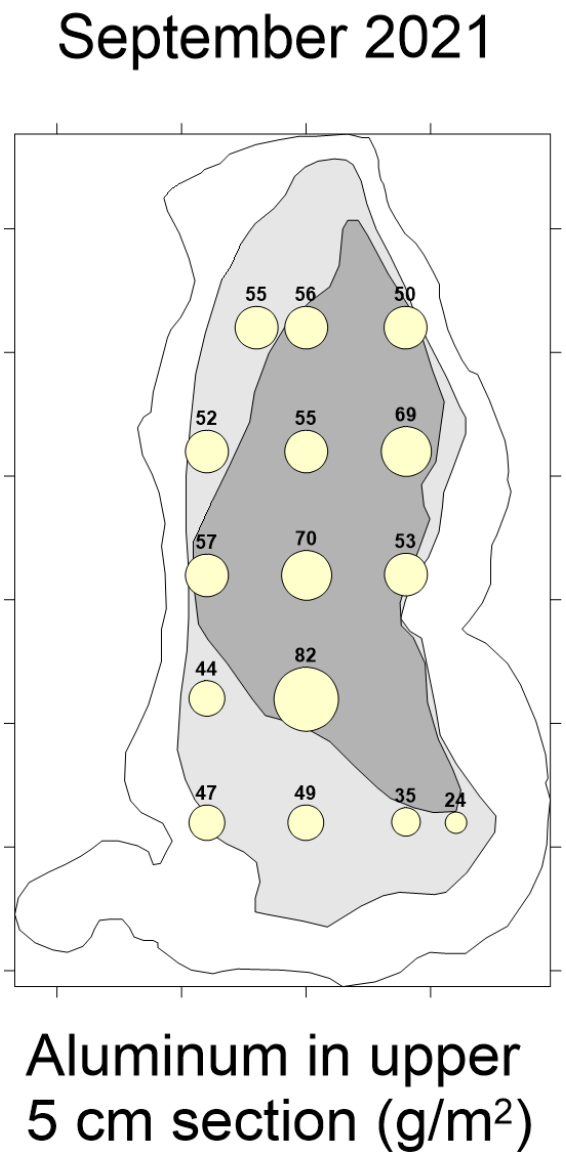

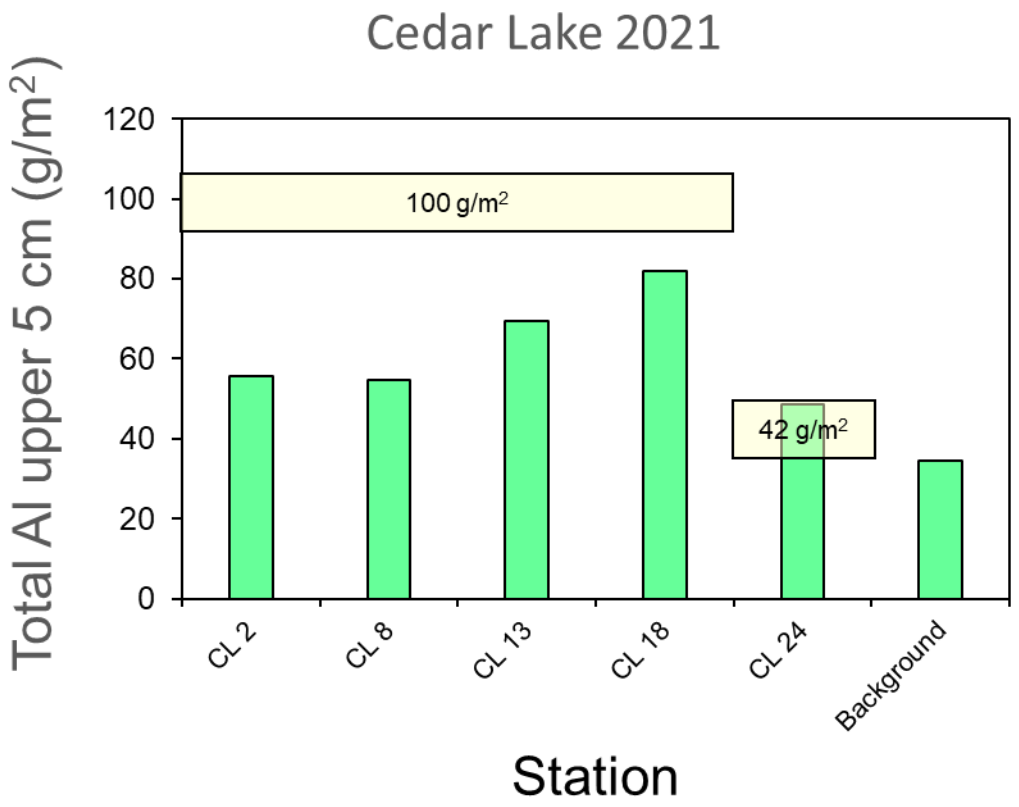

Figure 26. Variations in the estimated area-based sediment total aluminum concentration along the N-S longitudinal transect (see Figure 1) after the 3rd alum application in 2021. The area-based Al concentration was estimated based on the assumption that the Al floc layer was 5-cm in thickness and occupied the upper region to the sediment core slice. Background represents the Al concentration of the native sediment before the initiation of alum treatments.

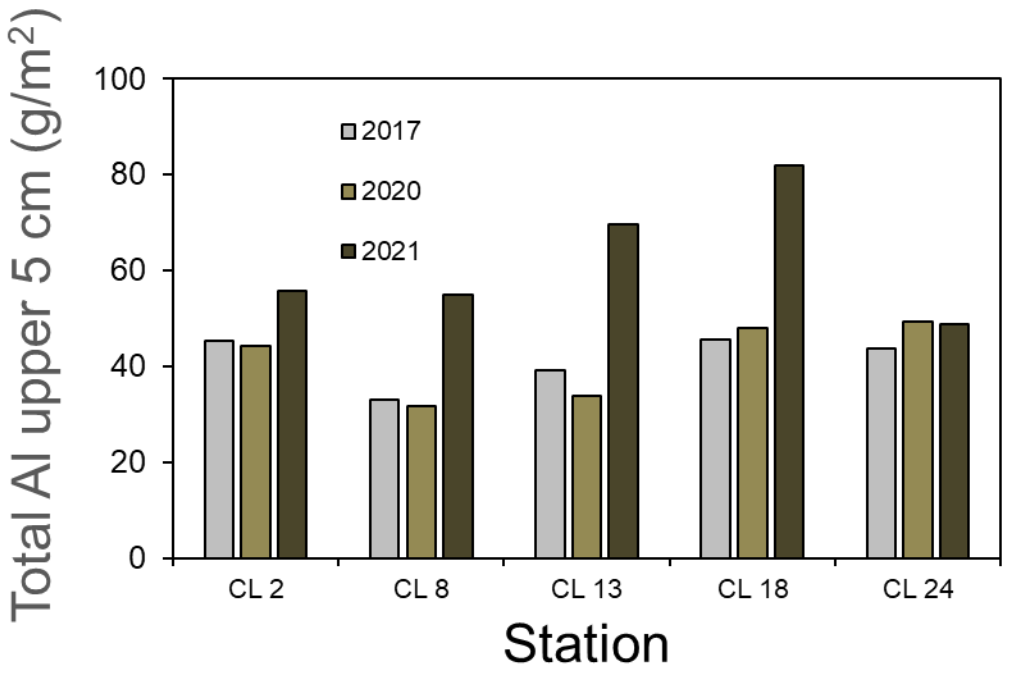

Figure 27. Time-series of variations in the estimated area-based sediment total aluminum concentration along the N-S longitudinal transect (see Figure 1) after the 2017, 2019, and 2021 alum applications. The area-based Al concentration was estimated based on the assumption that the Al floc layer was 5-cm in thickness and occupied the upper region to the sediment core slice. Background represents the Al concentration of the native sediment before the initiation of alum treatments.

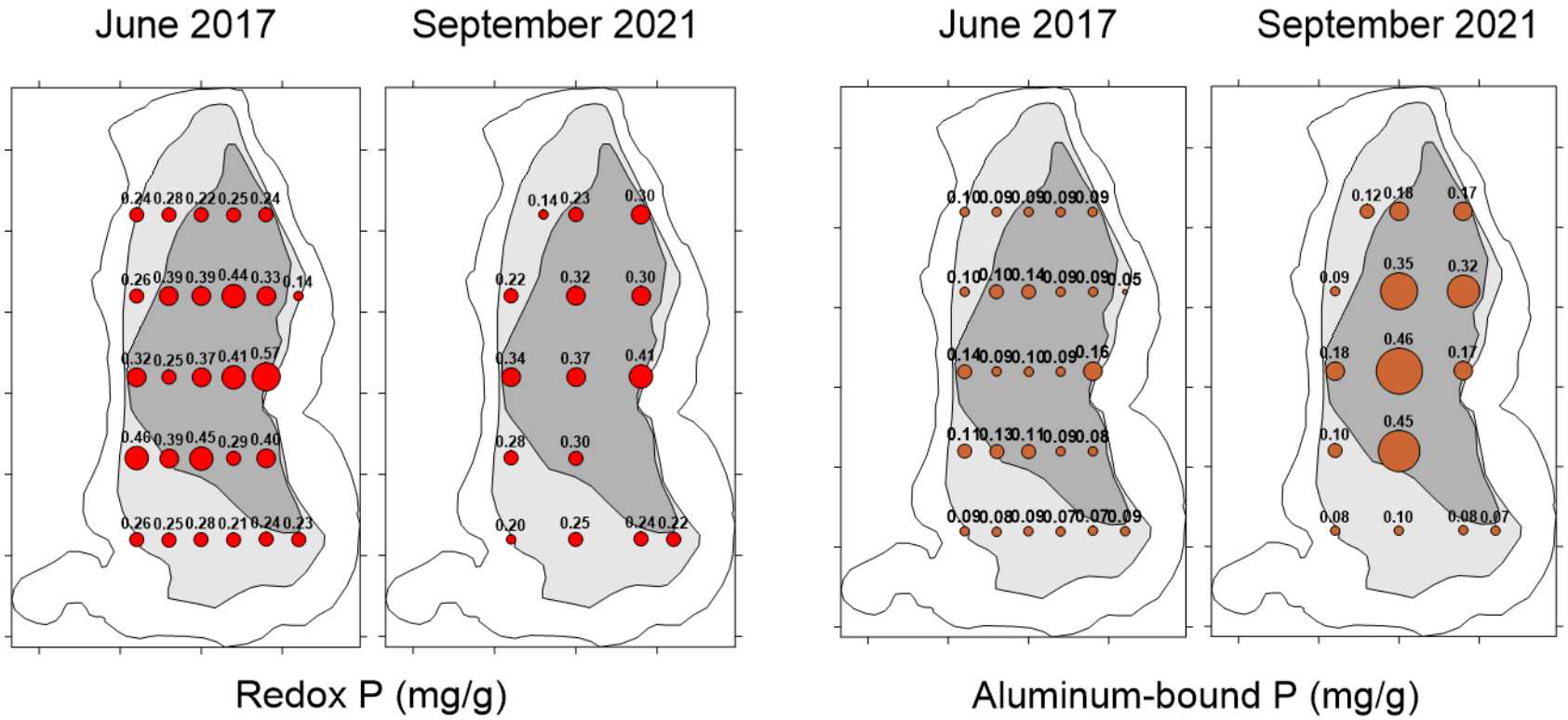

Figure 28. A comparison of spatial variations in surface sediment redox P (left panels) and aluminum-bound P (right panels) immediately before the initial alum treatment in 2017, after the 3rd alum application in 2021.

Figure 29. Vertical variations in sediment moisture content, wet sediment density, redox P (i.e., the sum of the loosely-bound P and iron-bound P sediment fractions) phosphorus (P), and aluminum (Al)-bound P concentrations for a sediment core collected from station WQ2 (Figure 1) in June 2017 and September 2021. The sediment profile in June of 2017 represents pre-treatment conditions while September 2021 represents post-alum treatment conditions after three alum applications (2017, 2019, and 2021).

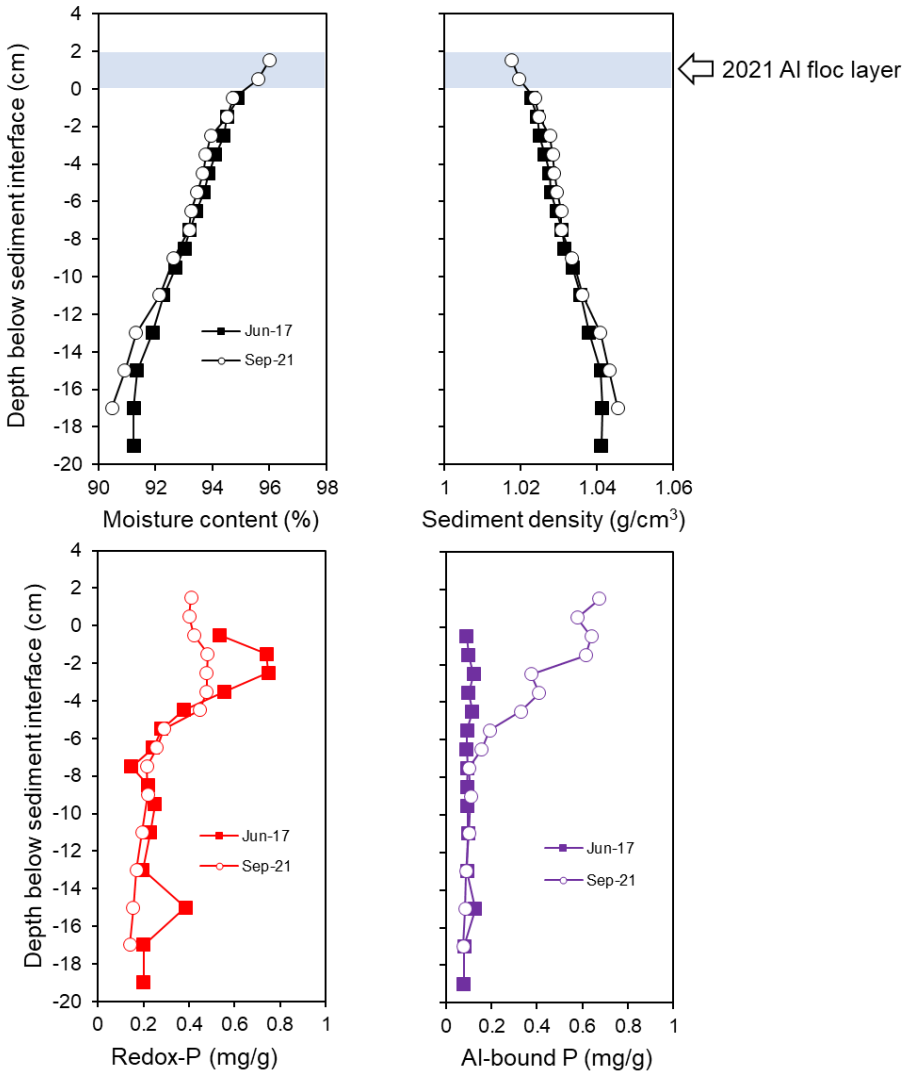

Appendix 1. Detailed vertical water column profiles of water temperature, dissolved oxygen, total P, soluble P, and chlorophyll for various dates in 2021.

- The lake developed strong stratification on 5/24 and 6/7
- Bottom dissolved oxygen declined to near zero on 5/24 and < 2 mg/L on 6/7
- Soluble P concentrations increased above the sediment-water interface starting on 5/10. Bottom concentrations peaked at near 0.04 mg/L on 5/24 Mixing and uptake by cyanobacteria occurred after 6/7.
- A modest subsurface chlorophyll concentration maximum developed immediately above bottom water SRP concentration gradients on 5/24. Water column mixing and entrainment of soluble P resulted in uptake by cyanobacteria. The algal population was ~ homogeneously mixed throughout the water column on 6/7 and 6/21. A subsurface chlorophyll concentration peak composed of cyanobacteria re-developed by 7/6 after lake stratification. The position of the subsurface cyanobacteria bloom was probably optimal for light radiation and photosynthesis.
- Bottom soluble P again increased in concentration with re-establishment of stratification and bottom anoxia (see next figure on page 47). The subsurface chlorophyll concentration peak was positioned immediately above these P concentration gradients.

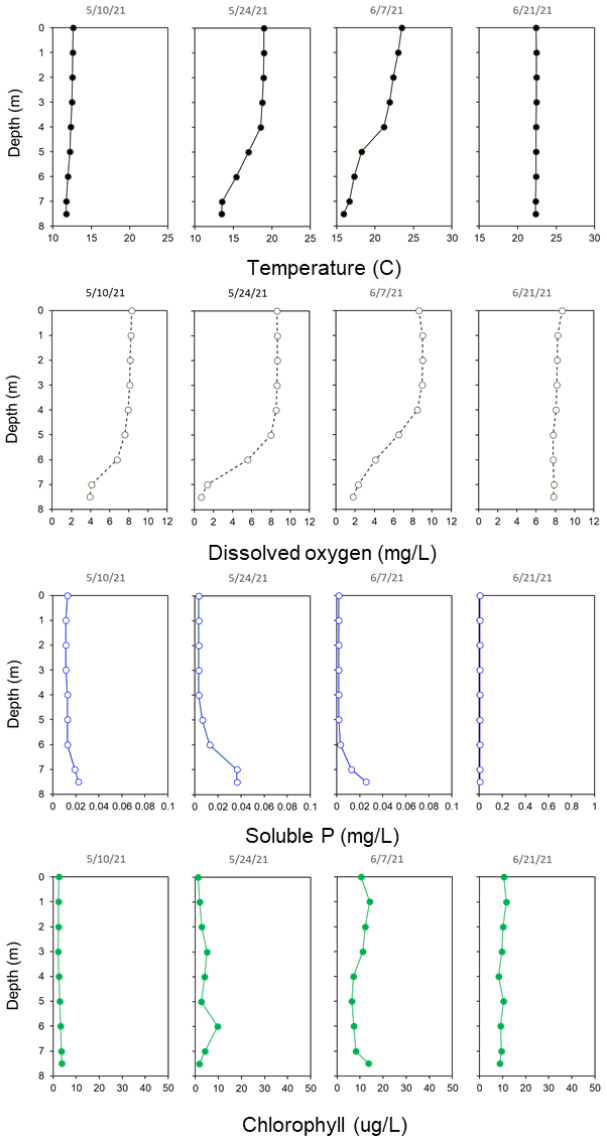

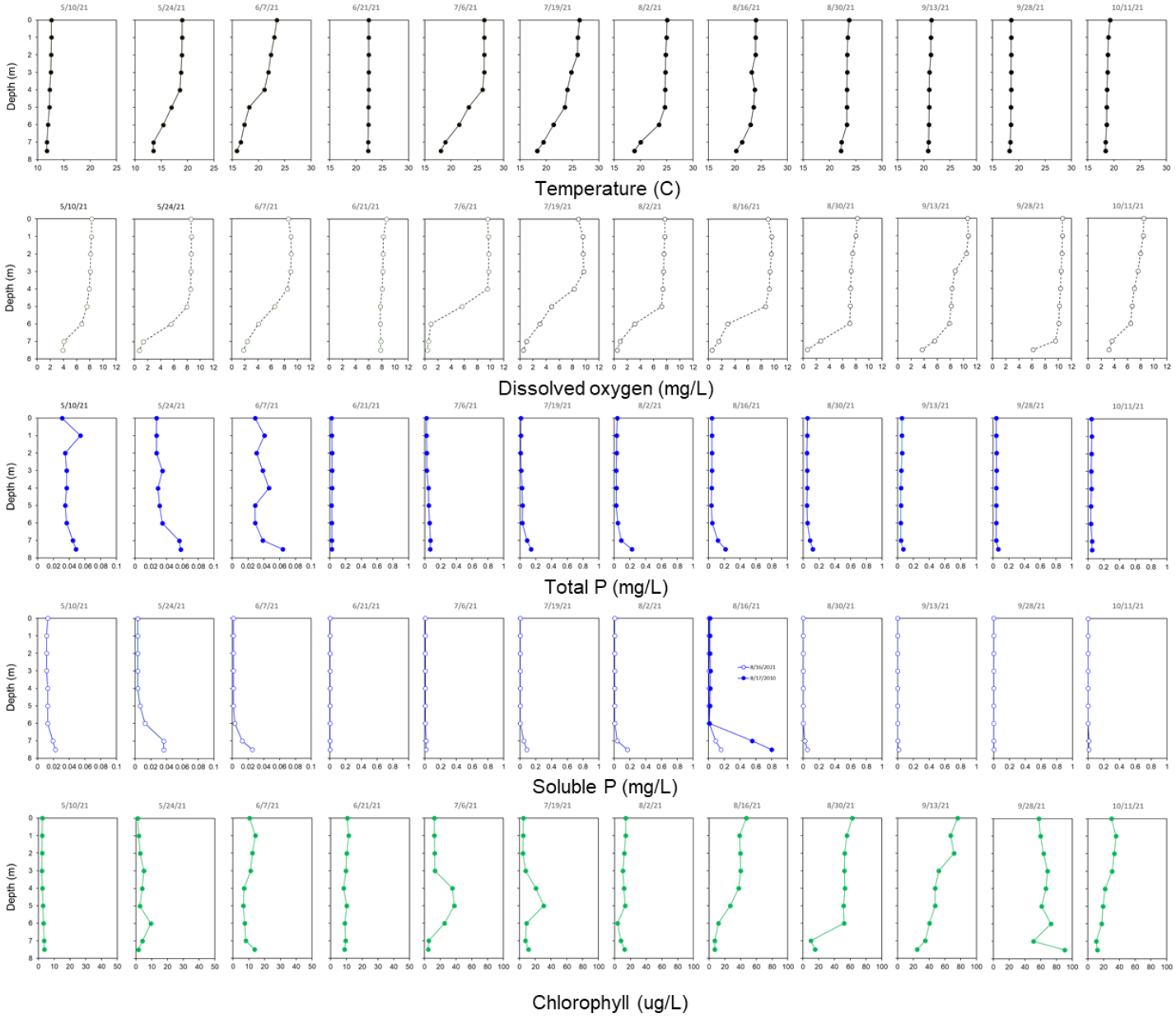
5/10/21
5/24/21
6/7/21
6/21/21
7/6/21
7/19/21
8/2/21
8/16/21
8/30/21
9/13/21
9/28/21
10/11/21
Depth (m)
Temperature (C)
Dissolved oxygen (mg/L)
Total P (mg/L)
Soluble P (mg/L)
Chlorophyll (ug/L)
8/16/2021
8/17/2010